Review

Modelling and Simulation of Effusion Cooling—A Review of Recent Progress

Hao Xia [1,*], Xiaosheng Chen [2] and Christopher D. Ellis [3]

[1] Department of Aeronautical and Automotive Engineering, Loughborough University, Loughborough LE11 3TU, UK
[2] Department of Engineering Science, University of Oxford, Oxford OX1 2JD, UK; xiaosheng.chen@eng.ox.ac.uk
[3] Mechanical, Materials & Manufacturing Engineering, University of Nottingham, Nottingham NG7 2RD, UK; chris.ellis.1@nottingham.ac.uk
* Correspondence: h.xia@lboro.ac.uk

Abstract: Effusion cooling is often regarded as one of the critical techniques to protect solid surfaces from exposure to extremely hot environments, such as inside a combustion chamber where temperature can well exceed the metal melting point. Designing such efficient cooling features relies on thorough understanding of the underlying flow physics for the given engineering scenarios, where physical testing may not be feasible or even possible. Inevitably, under these circumstances, modelling and numerical simulation become the primary predictive tools. This review aims to give a broad coverage of the numerical methods for effusion cooling, ranging from the empirical models (often based on first principles and conservation laws) for solving the Reynolds-Averaged Navier–Stokes (RANS) equations to higher-fidelity methods such as Large-Eddy Simulation (LES) and hybrid RANS-LES, including Detached-Eddy Simulation (DES). We also highlight the latest progress in machine learning-aided and data-driven RANS approaches, which have gained a lot of momentum recently. They, in turn, take advantage of the higher-fidelity eddy-resolving datasets performed by, for example, LES or DES. The main examples of this review are focused on the applications primarily related to internal flows of gas turbine engines.

Keywords: effusion cooling; cooling effectiveness; Reynolds-averaged Navier–Stokes equations; large-eddy simulation; hybrid RANS-LES; machine learning

1. Introduction

Cooling is critical in most heat engines, especially highly efficient gas turbines. Within the combustor of a modern gas turbine engine, either ground based for power generation or airborne for propulsion, the temperature of the hot gases as a result of the chemical reaction can be extremely high and can still reach above 1700 K even towards the downstream at the exit of the combustor. No metallic material or structure is likely to withstand such high temperatures without some form of protection. Among many cooling techniques, film cooling [1] is particularly effective under these conditions. A "film" of cooler air flow, if well distributed, can cover the critical metal components as the designer intended, hence providing vital protection against the aforementioned extremely hot environment. Despite the compressed cooling air temperature being typically around 500 to 800 K, which may seem to still be very hot, it is sufficiently low to protect the metal components from much hotter temperatures the components are exposed to.

As the schematic in Figure 1(left) shows, a coolant film is formed on the hot side of the metal to provide protection. Very often, a single hole or slot to allow for the coolant to pass would be quite limited as to its effectiveness and cooling efficiency. Achieving cooling protection, while avoiding some of the complex interactions of a jet-in-cross-flow (see Figure 2 below), can be challenging. This leads to the second concept in Figure 1(right), where the number of cooling holes is considerably increased with an array of closely

spaced holes, namely, the effusion cooling technique. Effusion cooling aims at providing cooling films fully covering the hot side of the solid surfaces. Theoretically, effusion cooling becomes transpiration cooling, when the hole diameter and the hole spacing are small enough. Practically, effusion cooling involves a perforated plate with multi-row holes, while transpiration cooling involves completely porous materials [2].
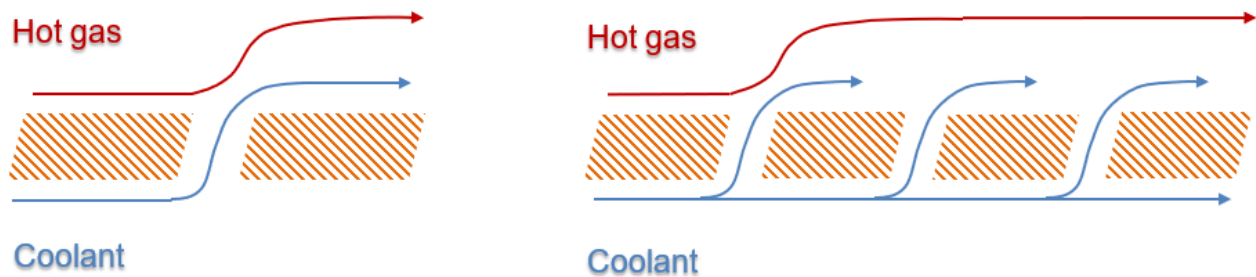

Figure 1. Illustrative concepts of film cooling (**left**) and effusion cooling (**right**).

Because the multiple cooling holes can be placed quite densely, the adjacent cooling jets interact with each other and form a fully covering cool film without the need to increase the jet momentum ratio, hence avoiding jet-in-cross-flow losses. This would directly translate to better protection and highly efficient use of coolant mass flows. For these reasons, effusion cooling is regarded as an advanced concept and technique for cooling the combustor liners and turbine blade in gas turbines [3]. As is shown later in this review, despite predominant applications of multi-hole effusion cooling in engineering practices, studies on single-hole arrangements provide more detailed analyses to improve understanding and modelling methods.

Experimental and computational studies of effusion cooling have been widely conducted due to the highly relevant industrial importance, and their publications can be quite easily found in the literature. There are also many review articles on the general subject of effusion cooling. For example, the review article of Wang et al. [2] gives an extensive account of advanced effusive cooling techniques for turbine blades. However, the motivation of the present review is to provide an up-to-date review that specifically focuses on the latest progress in computational efforts in predicting effusion cooling performances, of which some are among the authors' most recent work, which we believe is the first of its kind spanning a hierarchy of modelling and simulation methodologies. Conjugate Heat Transfer (CHT) is not particularly covered in this review simply because, by means of a dimensionless cooling effectiveness parameter, an adiabatic wall boundary condition is sufficient to assess the cooling performance. The paper is organised as follows. An overview of the numerical simulations is given first, and four sections of individual modelling/simulation methods and their representative results are presented next, followed by a further section on machine learning and data-driven techniques, before the conclusions.
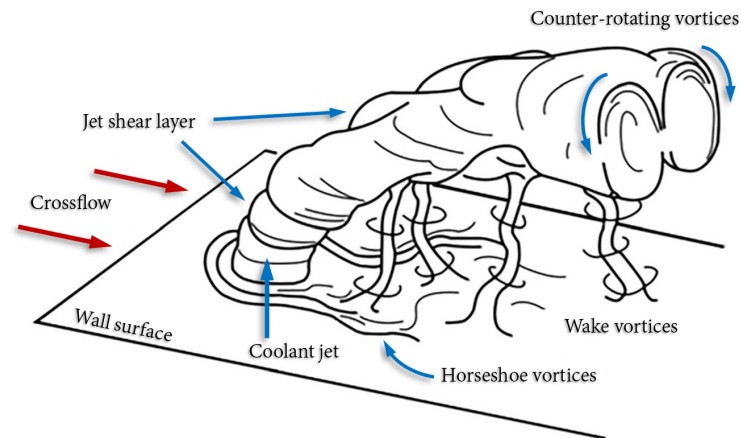
Figure 2. Fluid dynamicists' impression of a single circular coolant jet in a heated crossflow, inspired by [4]. Notice the presence of horseshoe and wake vortices may not be as strong at different jet angles.

2. Overview of Numerical Methods and Challenges

While the appearances of a film cooling or effusion cooling flow may vary depending on the configurations and flow conditions, such as Reynolds number (Re), density ratio, and blowing ratio, the essential flow features they all share can be summarised by those of a jet-in-cross-flow, as shown in the sketch of Figure 2. It can also be certain as shown in this review that the Reynolds number given under these conditions would be sufficiently high, and the turbulent flow regime is typically expected. This defines the challenges posed to the modelling/simulation methods, which need to deal with not only the turbulence modelling of the incoming boundary layer, but also jet mixing, separation, and turbulent transport of enthalpy.

To study such complex heat and mass transfer problems for potentially quite different configurations, the series of numerical methods vary in a hierarchy of fidelity and cost (see Figure 3 below). In the meantime, with the addition of machine learning and data-driven augmentation, higher-hierarchy methods such as DNS or LES also provide datasets to train new RANS models, as discussed in Section 7.

Despite the variety of methods, one key non-dimensional parameter has been at the centre of numerical predictions [1–3], which describes the effectiveness of cooling: the so-called Adiabatic Cooling Effectiveness (ACE), η_{ad}, as defined by:

$$\eta_{ad} = \frac{T_\infty - T_w}{T_\infty - T_c} \tag{1}$$

where T_∞ is the bulk temperature of the hot gas stream, T_w the wall temperature or the fluid temperature immediately next to the wall on the hot side, and T_c the coolant temperature. Clearly, one expects $0 \leq \eta_{ad} \leq 1$ [5–11]. In an idealised situation, where the coolant provides a perfect protection, $T_w = T_c$; hence, $\eta_{ad} = 1$. Conversely, if T_w is closer to T_∞, i.e., the cooling has not been effective, then $\eta_{ad} \to 0$. Although by its name, ACE appears to be a measurement only for an adiabatic wall, it actually reveals the performance of the convection and diffusion part of the heat transfer process even when the wall is conductive.

To the lowest fidelity end, experimental-data- and first principles-based empirical relations were first developed to solve a single-row effusion cooling problem. These attempts also included analytical methods looking at the control volume, employing mass and energy conservation. Streamline patterns can often be assumed to simply the problem. As discussed in more detail in Section 3, these methods have managed to produce reasonable results for single-hole geometries while struggling considerably more with multi-hole scenarios where spatial periodicity in the streamwise direction cannot be easily assumed, despite the fact that they are super fast [5–7].

Solving the RANS (Reynolds-Averaged Navier–Stokes) equations is the next level on the hierarchy triangle. RANS is a vast subject within turbulence modelling (see, for

example, [12]), which aims for statistical descriptions of the flow. It employs Reynolds decomposition and time-average to reduce the time-dependent Navier–Stokes equations to ones that look alike with additional closure terms—Reynolds stresses. Even with Unsteady RANS (URANS), the averaging time is still much larger than the largest timescale of the turbulent fluctuations, and as a result, one ends up with conservation equations that describe the evolution of the mean flow quantities only. However, most RANS models are calibration-reliant. The fact that a wide range of one-equation and two-equation models are based on the Boussinesq eddy viscosity hypothesis also means that, due to its questionable validity, accurate predictions for η_{ad} can be a challenge. Although RANS models not based on eddy viscosity can still perform relative well, they do suffer from stiffness of the extra equations of the model itself, such as Reynolds Stress Model (RSM) with up to nine more equations to solve for each spatial point; otherwise, RANS is generally viewed as being very efficient to solve.

In contrast to the time-averaging process in RANS, LES (large-eddy simulation) employs a spatial filtering process instead to remove the unresolvable scales by the grid size. Hence, subgrid scale stresses would need some kind of closure. However, unlike the RANS Reynolds stress tensor, the subgrid scale stress tensor only reflects the influence of small-scale turbulence on large-scale (grid-scale) flow quantities. Section 6 below gives a full account of the LES methods in predicting η_{ad}. The drawbacks of eddy-resolving LES are chiefly down to its unrealistic requirement of the number of grid points, $N \sim Re^{13/7}$, for practical applications [13]. As for the fully resolving DNS (direct numerical simulation), it is only applicable for very low Reynolds number cases, as the number of required grid points becomes $N \sim Re^{9/4}$ [14], even for a conservative estimate.

As its name suggests, a hybrid RANS-LES benefits from the hybridisation of RANS and LES; therefore, it is more affordable. The zonal hybrid methods are based on a discontinuous treatment of the RANS-LES interface, e.g., a fixed wall distance in y+ units. In practice, information must be exchanged at the RANS-LES interface between two solutions with different spectral contents. The global hybrid methods are based on a continuous treatment of the flow variables at the interface between RANS and LES. These methods, like DES (detached eddy simulation) [15], introduce a "gray area" in which the solution is neither pure RANS nor pure LES since the switch from RANS to LES does not imply an instantaneous change in the resolution level. Despite a wide number of approaches (and acronyms), these methods are quite similar and can very often be rewritten as variants of a small group of generic approaches. In practice, they tend to decrease the level of RANS eddy viscosity, thus permitting strong instabilities to develop. It is now commonly accepted that hybrid RANS-LES is the main strategy to drastically reduce computational cost (compared with LES) in a wide range of complex industrial applications including effusion cooling if attached boundary layers have a significant impact on the global flow dynamics. In Section 5, the hybrid methods are fully discussed in further detail.

It is only very recently that high-fidelity methods, such as LES (or DNS), found another great application—to create machine learning (ML) datasets (although often involving higher-order statistics) for training augmented RANS models. Evidently, this fascinating new subject benefits from the latest development of Artificial Intelligence (AI) and data science, such as Artificial Neuron Network (ANN), which this review also covers towards the end.
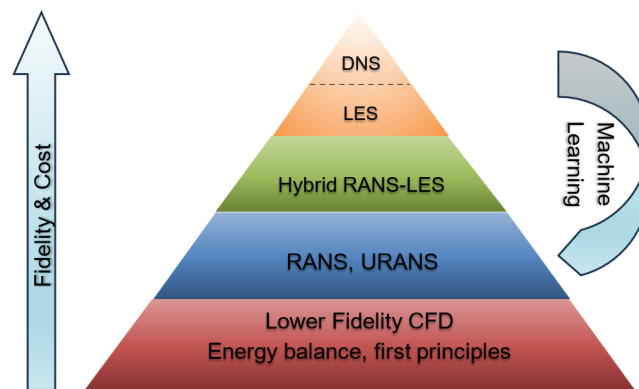
Figure 3. Hierarchy of fidelity and cost of CFD methods.

3. Semi-Analytical Modelling

3.1. Single-Hole Models

Detailed coolant film formation mechanisms for effusion cooling applications vary with different hole designs and array configurations owing to the jet-to-mainstream and jet-to-jet interactions. But the fundamental flow physics for a single-hole application is well investigated and summarised as a jet-in-cross-flow.

A number of works carried out in the pre-70s of the last century explored different types of the film or effusion cooling methods, trying to maximize the ACE. The first paper that summarised all the early works of the jet-in-crossflow type of cooling methods, including some simplified analytical or semi-empirical models to predict the ACE, was presented by Goldstein in 1971 [1]. An analytical method using the overall energy and mass conservation based on the control volume concept was introduced, as Figure 4 shows.
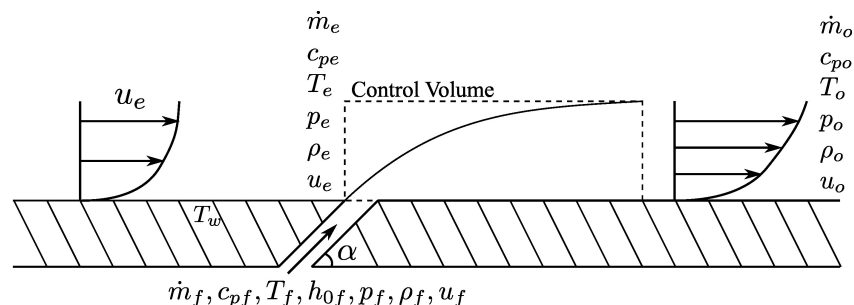

Figure 4. A sketch of the control volume method described by Goldstein [1].

Baldauf and his colleagues [16] presented an empirical solution for the single-row film cooling effectiveness based on the experimental data. They divided the flow into two regions, as Figure 5 illustrates: the first one is a complex flow domain with a strong 3D character located very close to the coolant exit, whilst the second one is located further in the downstream region where a diluting coolant film with 2D characteristics is identified. The cooling effectiveness was estimated in the second region using the control volume analysis and damping functions, in which the correlations were established based on the experimental data.
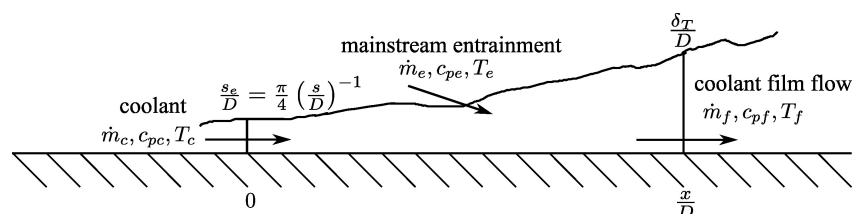

Figure 5. A sketch of the coolant film development theory by Baldauf and his colleagues [16].

LeGrives [17,18] developed another semi-analytical method and identified two mechanisms controlling the film cooling effectiveness. As Figure 6 suggests, LeGrives explained that the dilution process includes not only the mixing of the coolant jet by turbulent diffusion, but also the entrainment of the external mainstream by the vortices. Extensive measurements, flow visualisations, and derivation attempts were carried out by LeGrives, who determined an expression for the mass entrainment ratio. Meanwhile, the turbulent diffusion and entrainment due to the spreading of the jet was derived from the empirical expressions by Keffer and Bains [19].
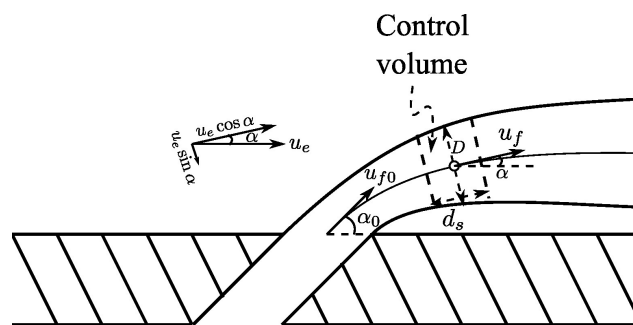

Figure 6. A sketch of the semi-analytical method proposed by LeGrives [17,18].

The work by Chen [5] utilised the analytical and semi-analytical models above to make comparisons with the experimental results by Sinha [20] and a hybrid LES study. It was found that those analytical models could predict the level of ACE in the far wake region ($x/D > 8$) but are completely wrong in the near wake region. These models might be a good tool to estimate the applications of film cooling where the holes are relatively large and separated, but they cannot be used for effusion cooling applications where the coolant holes are small and compact.

3.2. Superposition Models

As explained previously, the difficulty of theoretically predicting the cooling effectiveness of effusion cooling applications is the smaller, more compact, and interacting coolant jets. Since the 1970s, numerous attempts have been made to establish a model that extrapolates results from much smaller measurements or calculations for the prediction of the cooling effectiveness in effusion cooling applications.

In Sasaki et al.'s work [21], they compared the experimental results of a multi-row effusion cooling application with Sellers' superposition model [22] from single-hole results. They suggested that the superposition model is only able to provide good agreement in a far wake region ($x > 3D$) and only when the holes are laterally widely spaced.

The superposition method is also developed for predictions that evolve conjugate heat transfer (CHT) in effusion cooling cases to combine the heat convection in the fluid with conduction within the solid wall. The implemented heat sink method proposed earlier by Mayle [23] was used in a full-coverage effusion cooling study performed by Eckert in 1984 [24]. The blade leading edge was cooled by 11 rows of cooling holes, and heat transfer coefficients were calculated from measurements of adiabatic wall temperature. The analytical model did not give satisfactory results compared to the measurements. Recently, Arcangeli et al. [25] developed a simplified 2D conjugate approach to calculate the cooling effectiveness of an effusion cooled plate based on correlations from experimental results. For the conjugate plate, a good parabolic correlation was derived between the coolant mass flow rate and cooling effectiveness, but it does not work for adiabatic walls. Moreover, as the authors stated, the correlation only works for certain input parameters similar to their experimental conditions. The universality has not yet been demonstrated.

The research team of Crawford et al. [26,27] chose another approach of using an injection model with an adjusted turbulent mixing length. This model was tested by experimental data of a flat copper plate with a fixed hole size at different injection angles,

blowing, and density ratios. The model predicted the downstream region of the first few rows well despite the transition region. However, this model only works for low blowing ratios and failed to provide reliable results at high blowing ratios.

Andreini and his colleagues at the University of Florence explored the semi-analytical model for the multi-hole effusion cooling case in the early 2010s [28,29]. They started with experimental measurements of effusion-cooled multi-perforated plates representing the combustor liner [28]. Some analytical work was carried out to establish, in an indirect way, the augmentation of the hot-side heat transfer coefficient due to effusion jets. Later, they carried out some RANS simulations [29] on a 3-million-cell wall-resolving grid using Menter's *k-ω* Shear Stress Transport (SST) model in ANSYS CFX. It is worth noting that they also simulated the thermal conduction within the plate between the hot and cold sides for the purpose of developing a lower-order heat sink model for CHT prediction.

Although the need for analytical or semi-analytical models has decreased with rising computational power, engineering design still benefits from those simplified or lower order models, especially when determining the arrangement of hundreds of coolant holes in a combustor liner. Unfortunately, none of the models presented so far provide satisfactory accuracy and universality in cooling effectiveness predictions.

4. Reynolds-Averaged Navier–Stokes Modelling

The RANS modelling of single- and multi-hole cooling flows is well-featured within the literature. Broadly, numerical studies from linear two-equation turbulence models to Reynolds stress models have been explored to close the Reynolds stress term. However, studies of turbulent heat flux closures are less diverse, and in earlier work, the closure method is often not discussed, but it was common practice to use the Gradient Diffusion Hypothesis (GDH) or its variations such as Higher-Order Generalised GDH (HOGGDH), as it was analogous to the treatment of turbulent diffusivity in the momentum transport equation. Articles that explore alternative methods are also summarised in the present section. A table summarising the reviewed RANS cases is provided in Table 1.

Table 1. Table of reviewed RANS cases with investigated turbulence modelling approaches.

Paper	Year	Turbulence Models	Turbulent Heat Flux
Bergeles et al. [30]	1978	Wall anisotropy model *	
Leylek and Zerkle [31]	1993	Standard *k-ε*	
Walters and Leylek [32]	1996	Launder–Spalding *k-ε* High Re	
Walters and Leylek [33]	1996	Launder–Spalding *k-ε* Two-layer	
Ferguson et al. [34]	1998	Standard *k-ε* two-layer wall model RNG *k-ε* RSM *	
Hoda and Acharya [35]	2000	High Re *k-ε* Low Re *k-ε* Launder–Sharma Lam–Bremhost model Low Re *k-ω* DNS-based Low-Re *k-ε* Low-Re Mayong–Kasagi * Speziale *	
Acharya et al. [36]	2001	*k-ε* RSM *	
Azzi and Jubrain [37]	2003	*k-ε* with wall-based anisotropy model *	
Harrison and Bogard [38]	2008	Realizable *k-ε* Standard *k-ω* RSM *	
Li et al. [39]	2015	Algebraic anisotropic eddy viscosity model	Anisotropic scalar flux with GDH and HOGGDH
Ling et al. [40]	2016	Pseudo RANS with LES fields	GDH ($Pr_t = 0.85, 0.6$) GDH (α_t from LES) HOGGDH ($C = 0.6, 1.5$)

Table 1. *Cont.*

Paper	Year	Turbulence Models	Turbulent Heat Flux
Laschet et al. [41]	2002	Algebraic eddy viscosity model [42] *	
Bohn and Krewinkel [43]	2009	Algebraic eddy viscosity model [42] *	
Ceccherini et al. [44]	2008	*k-ε* with wall-based anisotropy model [37] *	
Ceccherini et al. [45]	2010	SST Menter *k-ω*	
Andreini et al. [46]	2010	SST Menter *k-ω*	
Coletti et al. [47]	2013	Standard *k-ε*	GDH ($Sc_t = 0.85$)
Andrei et al. [48]	2014	SST Menter *k-ω* with wall-based anisotropy model [37] *	
Ledezma [49]	2016	SST Menter *k-ω* with enhanced wall functions Realizable *k-ε* with enhanced wall functions	
Krawciw [50]	2017	Two-layer realizable *k-ε* model	GDH

* non-linear models.

4.1. Single Hole

Leylek and Zerkle [31] used RANS modelling with the standard *k-ε* model and the generalised wall function treatment of Launder and Spalding [51]. The closure of the turbulent heat flux term was not discussed in the article. This early study supplied extensive results compared to the experimental studies of Pietyzk et al. [52,53] and Sinha et al. [20]. Predictions of centreline cooling effectiveness did not predict the trends associated with jet detachment and the lateral coolant spreading behaviour was underpredicted compared to the experiment. Exit plane velocity profiles were shown for various blowing ratios and coolant hole length-to-diameter ratios, which revealed highly skewed velocity profiles for different conditions. This raised the importance of accurately replicating the coolant hole flow to replicate combustor and turbine geometrical conditions.

Seven turbulence modelling approaches, considering generalised and non-equilibrium wall functions, were compared on a single-hole cooling geometry by Ferguson et al. [34]. A standard *k-ε* model including a two-layer wall treatment, a Re-Normalisation Group (RNG) *k-ε* model, and RSM were explored. The results showed that the linear *k-ε* model performed better than the non-linear RSM, with improvements observed in the modelled turbulence level. The selection of near-wall treatment was crucial where only the two-layer wall treatment was able to predict the separation bubble that occurred due to coolant jet lift-off.

Turbulence models and their predictions of the film cooling jet-in-crossflow case were studied by Hoda and Acharya [35]. Seven different models were studied: High-Re *k-ε*, Low-Re formulation of the *k-ε* Launder–Sharma model and Lam–Bremhost model, Low-Re *k-ω* model, DNS-Based Low-Re *k-ε*, and the non-linear Low-Re Mayong–Kasagi model and Speziale model. The High-Re *k-ε* model overpredicts values in spanwise and vertical velocities and is not recommended for complex flows. Near-wall flow is well predicted by the Launder–Sharma model, but it fails to capture trends in turbulent mixing within the jet wake. Likewise, the Lam–Bremhost model predicts accurate near-wall behaviour but predictions in the jet do not agree with the validating experiment, and it fails to predict the recirculation ahead of the jet. The DNS-based *k-ε* model scales correlation terms for an *ε* budget calculated from the DNS of a channel. However, this simplified budget fails to predict the correct gradients in the spanwise and streamwise directions within the jet and wake, but the recirculation is well captured by the DNS-based *k-ε* model. Both non-linear models show inconsistencies when compared to the experimental data, with the Speziale model unable to predict the trends seen in the jet and wake, while the Mayong–Kasagi model overpredicts the vertical penetration of the jet. These predictions are thought to be a consequence of how the model is fitted to simple wall-bounded flows. The *k-ω* model provides reasonable predictions of the near-wall flow.

A later study by Acharya et al. [36] investigated *k-ε* models and an RSM, comparing the results to the experimental, LES, and DNS data. Observations indicated that jet exit boundary conditions are critical to numerical predictions and the boundary should be

derived from experiments, or the jet hole and plenum should be modelled. The two-equation models were seen to overpredict the coolant penetration and underpredict the jet's lateral spreading as a result of the linear eddy viscosity model. RSM calculations showed only marginal improvements over the two-equation models. Critically, it is often presumed that the RSM provides realistic anisotropy; however, it is demonstrated that the modelling of each Reynolds stress transport equation can dampen the desired anisotropy of the complex flow. Finally, Acharya et al. [36] showed that the LES and DNS calculations provided a better prediction of the mean velocities and the turbulent stresses.

Early computational studies by Walters and Leylek [32,33] aimed to replicate the ACE results of Sinha et al. [20] for a density ratio of 2.0 and blowing ratios of 0.5, 0.8, and 1.0. An unstructured grid with second-order spatial schemes was used with turbulence modelled by the Launder and Spalding standard k-ε turbulence model with High-Re wall functions. For the lower blowing ratio, correct trends in centreline effectiveness were seen, but their values were overestimated. At high blowing ratios, an overestimation was observed, and the effects of jet lift-off were not present in the centreline ACE. Corrections were used to account for the skew in the jet's centreline, which better captured the centreline and lateral cooing effectiveness in the downstream regions. Like Acharya et al. [36], the author commented on the lack of non-linear anisotropy in the modelled turbulence and its effect on the lateral coolant spread. Secondly, Walters and Leylek [32] commented on the requirement of low-Re or two-layer wall models to improve the numerical simulation of jet lift-off and reattachment. Further work by Walters and Leylek [33] showed that a two-layer model does not improve the cooling results in the downstream region, but improvements were seen in the recirculating flow immediately in the downstream of the hole.

Similarly, Harrison and Bogard [38] investigated the realizable k-ε, standard k-ω, and RSM turbulence models for predictions of heat transfer coefficients and ACE. All models showed poor predictions of coolant lateral spread, including the RSM, agreeing with the conclusions of Acharya et al. [36]. Results of ACE at a blowing ratio of 0.5 revealed that the standard k-ω provided the most accurate predictions of laterally averaged ACE but failed to predict the centreline effectiveness data. The realizable k-ε model presented opposing results where reasonable estimations of centreline ACE were observed while predictions of laterally averaged ACE were poor. At high blowing ratios, where cooling jet lift-off was present, all models performed poorly. The surface heat transfer coefficients showed underpredictions in the centreline values and overpredictions in lateral values for all three models.

Bergeles et al. [30] conducted a set of numerical studies providing accurate results for single cooling holes at small blowing ratios. An anisotropic model of Reynolds stresses was proposed to capture the complex turbulence. Equations (2)–(4) alongside the k-ε model closed the turbulent Reynolds-stresses and heat flux. The wall-normal Reynolds stress ($\overline{v'^2}$) was set to $k/3$, which provided a close fit over the inner boundary layer. Equation (2) fitted Quarmby and Quirk [54,55] data for radial to tangential diffusion ratios in pipe flow, where the parameter Δ is the boundary layer height and the streamwise velocity is equal to 95% of the freestream velocity. The derivation of the model was discussed in detail by Bergeles et al. [30]. The results showed suitable accuracy for a limited range of blowing ratios from 0.1 at a $90°$ injection angle to 0.5 at a $30°$ injection angle.

$$\frac{\nu_{t,z}}{\nu_{t,y}} = \frac{\alpha_{t,z}}{\alpha_{t,y}} = \begin{cases} 1.0 + 3.5\left(1 - \frac{y}{\Delta}\right) & y \leqslant \Delta, \\ 1.0 & y > \Delta \end{cases} \tag{2}$$

$$\nu_{t,y} = 0.09\frac{k^2}{\varepsilon}, \quad \alpha_{t,y} = 0.1\frac{k^2}{\varepsilon} \tag{3}$$

$$\overline{u'v'} = -\nu_{t,y}\frac{\partial U}{\partial y}, \quad \overline{u'w'} = -\nu_{t,z}\frac{\partial U}{\partial z} \tag{4}$$

Azzi and Jubran [37] applied the anisotropic model proposed by Bergeles et al. [30] to the standard *k*-*ε* model with wall treatments. For the low-blowing ratio case, the modification better captured the centreline ACE and lateral spreading when compared to the original model and the studies of Walters and Leylek [32]. At a larger blowing ratio, the model failed to predict the jet lift-off and reattachment that resulted in the differences from the experimental ACE in agreement with Bergeles et al. [30].

Ling et al. [40] assessed turbulent heat flux closures in a single-hole configuration using a pseudo-RANS computation, where the flows velocity and pressure were taken from the LES simulation of Bodart et al. [56], and a Reynolds-averaged advection–diffusion equation was used to solve the non-dimensional temperature field. GDH and HOGGDH closure models were assessed within the advection–diffusion equation to identify their impact on the surface cooling performance, with coefficients outlined in Table 2 with their respective non-dimensional temperature mean error. It was found that the HOGGDH model marginally improved the cooling prediction with a coefficient of 1.5 and the lateral coolant spread was in better agreement with the experiment. However, the authors found that using an LES-derived turbulent diffusivity provided the lowest error, but the contours of the cooling effectiveness did not capture the correct lateral coolant spread.

Table 2. Cases and respective errors for turbulent heat flux closures investigated by Ling et al. [40].

Case No.	Model	Parameter Value	Error
1	GDH	$\alpha_t = \alpha_{t,LES}$	0.013
2	GDH	$Pr_t = 0.85$	0.034
3	GDH	$Pr_t = 0.6$	0.023
4	HOGGDH	$C_{HOGGDH} = 0.6$	0.031
5	HOGGDH	$C_{HOGGDH} = 1.5$	0.020

Li et al. [39] developed an algebraic anisotropic turbulence model to improve the RANS predictive capability of gas turbine film cooling flows (Figure 7). An anisotropic eddy viscosity tensor was formed for use with the Boussinesq Hypothesis closure for Reynolds stresses. Anisotropic ratios used within the tensor were expressed using the algebraic Reynolds Stress transport equations. The scalar turbulent flux was manipulated similarly, utilising an anisotropic scalar–flux ratio based on the commonly used GDH and HOGGDH. The results of the centreline ACE showed improved agreement with the experimental data over the standard *k*-*ε* model. For flows with a high BR, the jet lift-off was still not captured, as ACE centreline trends differed close to the cooling hole. Spanwise-averaged cooling effectiveness results presented minor improvements over the standard *k*-*ε* model.
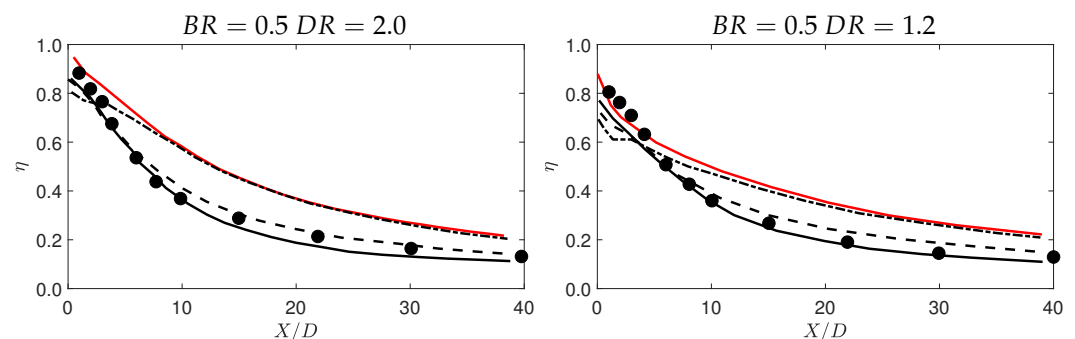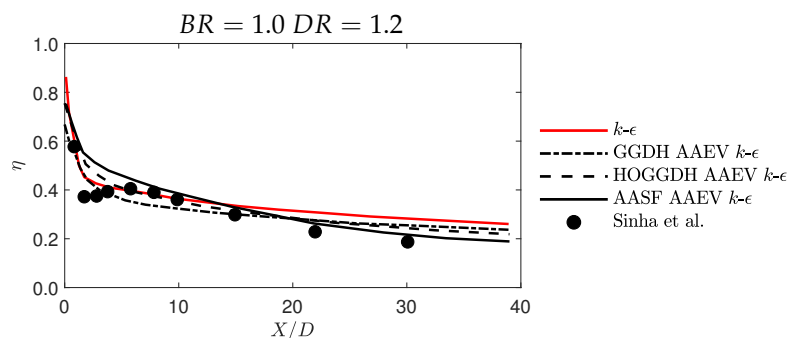

Figure 7. *Cont.*

Figure 7. Improved centreline ACE using the anisotropic model of Li et al. [39] (AASF AAEV *k-ε*). Adapted from Int. J. Heat Mass Trans., Vol. 91, Li et al. [39], Application of algebraic anisotropic turbulence models to film cooling flows, published by Elsevier.

4.2. Multi-Hole

Laschet et al. [41] investigated flow through a multi-perforated plate with conjugate heat transfer. An in-house CHT-fluids code was used with direct coupling between the heat transfer in the solid and the fluid flow using a common wall temperature. In the flow, a local 1D Riemann problem was solved on each cell face with a third-order accurate van Leer's MUSCL scheme with added diffusivity for stability. Viscous fluxes were discretised with a central differencing scheme, and the turbulence was modelled with Baldwin and Lomax's [42] algebraic eddy viscosity model. The results of the study showed that a fan-shaped cooling hole geometry led to a reduction in the thermal gradients in the solid. Further work by Bohn and Krewinkel [43] used the same approach as Laschet et al. [41] to investigate two different multi-layer material systems to optimise the longevity of the thermal barrier coating. Fan-shaped and cylindrical cooling holes were investigated for low blowing ratios of 0.28 and 0.48.

Numerical work using the anisotropic model from Azzi and Jubran [37] was performed alongside experimental work by Ceccherini et al. [44]. The anisotropic model provided a better agreement for the experimental study than a turbulence model with a standard two-layer wall function, although an overestimation of peaks and an underprediction of coolant lateral spread were still present. Later work by Ceccherini et al. [45] on combined slot and effusion cooling used the SST Menter *k-ω* turbulence model for ACE predictions. The results showed that the model overestimated the cooling effectiveness, and the shape of the trends was not seen.

Andreini et al. [46] investigated the heat transfer coefficients of the slot and effusion-cooled case of Ceccherini et al. [45]. RANS simulations were conducted with the SST Menter *k-ω* turbulence model. The authors highlighted the commonly observed overprediction of a coolant along the jet centreline and the underprediction of lateral spreading obtained with RANS approaches while the spanwise averaged prediction showed positive results. This is reflected in the work presented, with large differences in spanwise distributions. However, the spanwise-averaged results presented are in close agreement with the experiment.

The near-wall anisotropy model featured in Azzi and Jubran [37] was also used by Andrei et al. [48] with a *k-ω* SST turbulence model in the numerical portion of their article on multi-hole effusion cooling. An 18-row staggered cylindrical cooling hole arrangement was investigated at density ratios of 1.0 and 1.5 and blowing ratios of 1.0, 2.0, and 3.0.

Following the experimental portion of the paper by Coletti et al. [47], a RANS study using a standard *k-ε* model is shown. It was observed that both the position and the strength of the counter-rotating vortex pair were not properly captured. The local minima of the eddy viscosity between the counter-rotating vortex pair immediately after injection were not seen. Coolant concentrations were overestimated across the wall. To address the model discrepancies, the authors identified that a spatially varying Schmidt number would capture trends in the turbulent diffusivity observed in the experiments.

Krawciw investigated computational studies of effusion cooling arrays [50]. Comparisons were made between cylindrical, spey fan, modified fan, slotted, cylindrical, and rectilinear helix -shaped cooling holes (shown in Figure 8) at blowing ratios of 3.32 and 14.94 and freestream turbulence intensities of 5% and 20%. Simulations were conducted in Star-CCM+ using a two-layer realizable *k*-*ε* model for the Reynolds stresses, while the turbulent heat flux was closed with the GDH model. An unstructured polyhedral mesh with prism layers at the wall was used. Results for the cylindrical cooling hole cases were not comparable to the experiment and underpredicted the cooling effectiveness across the surface. Results for the other shaped holes, which provided an increased spreading effect at the injection point, were more comparable to the presented experiments but lacked the correct lateral coolant spreading as reported with the GDH approach.

Alongside an LES computational study, Ledezma [49] conducted RANS simulations with the *k*-*ω* SST and realizable *k*-*ε* turbulence models with enhanced wall functions for blowing ratios of 0.6, 0.8, and 1.0 for an eight-row multi-hole effusion cooling plate. The laterally-averaged cooling effectiveness results published showed that both RANS models underpredicted the cooling effectiveness while the LES results were comparable to the experiment. Cooling effectiveness contours showed that both RANS models did not accurately capture the lateral coolant spread observed in the experiment and LES results.
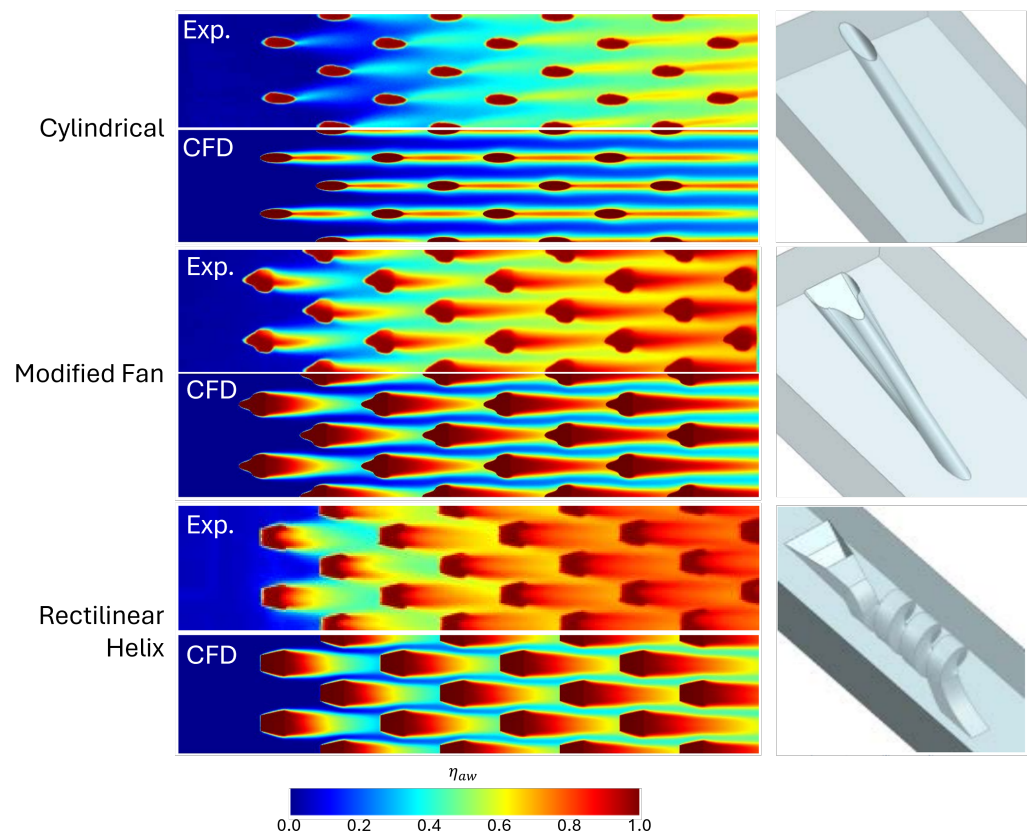

Figure 8. A sample of cooling effectiveness results from Krawcwiw [50] for varying effusion cooling hole geometries. Reprinted from Krawciw [50], Optimisation techniques for combustor wall cooling, published on the Loughborough University repository under the terms of a CC BY-NC-ND 4.0 license.

5. Hybrid RANS-LES

Due to the high near-wall resolution requirement of the full wall-resolving LES, hybrid RANS-LES methods have attracted more attention and interests in the last decade. A few researchers have been using it to model effusion cooling flows in single- and multi-hole cooling configurations.

Figure 9 presents a snapshot of turbulent structures and coolant-hole centre-plane vorticity field simulated by a zonal hybrid RANS-LES method, suggesting its ability to reproduce flow mixing between the hot mainstream and coolant jets. This section introduces some of the recent studies using hybrid LES modelling approaches for single- and multi-hole effusion cooling. A table summarising the reviewed hybrid RANS-LES cases is provided in Table 3.
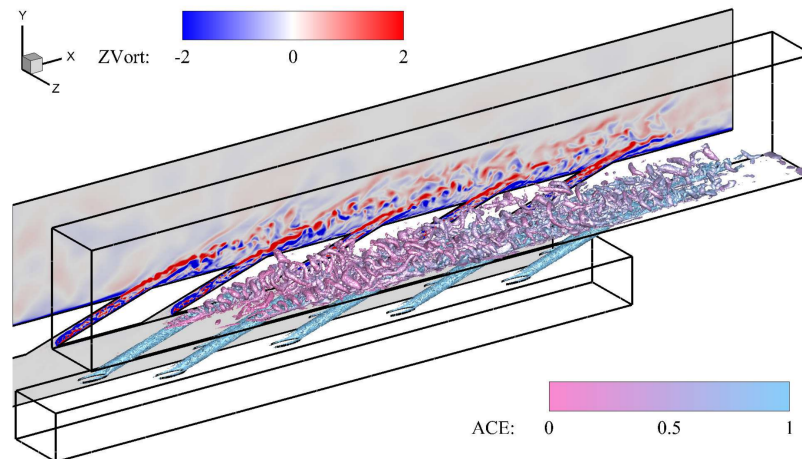

Figure 9. Visualisation of a multi-hole effusion cooling array from a hybrid RANS-LES study. Reprinted from Appl. Therm. Eng., Vol. 184, Chen et al. [7], Study of an effusion-cooled plate with high level of upstream fluctuation, published by Elsevier; CCC license for re-use obtained.

Table 3. Table of reviewed hybrid RANS-LES cases including information of turbulence models and inflow turbulence generation models.

Paper	Year	Turbulence Models	Turbulent Inflow Model
Roy et al. [57]	2009	SA-DES	–
Foroutan and Yavuzkurt [58]	2015	realizable *k-ε*-based DES	–
Chen and Xia [5]	2018	SST-based implicit LES	SEM
Jin et al. [59]	2022	*k-ω* based VLES	NA
		LES-WALE	NA
		SST-based DES	NA
Zamiri et al. [60]	2020	LES-WALE	NA
		SST-based SAS	NA
		DES	NA
Mazzei et al. [61]	2015	SST-based SAS	NA
		SST-based DES	NA
Mazzei et al. [62]	2016	SST-based SAS	NA
Lenzi et al. [63]	2020	SST-based SBES	NA
Arroyo-Callejo et al. [64]	2016	DRSM	NA
		SA-based Zonal DES	NA
		k-ω SST	NA
Chen and Xia [5–7]	2018–2021	SST-based implicit LES	SEM
		k-ω SST	NA

5.1. Single Hole

The first study that utilised a hybrid LES approach in single-hole cooling research was conducted by Roy and his colleagues [57]. They used a Spalart—Allmaras-based DES model on a film-cooled flat plate with unstructured grids. The 35-degree inclined coolant jet with a blowing ratio of 1.0 and density ratio of 2.0 was well predicted and greatly enhanced the description of the anisotropic mixing process. However, the laterally averaged film cooling effectiveness from the DES simulation failed to show much improvement than that

of the RANS model, which was attributed to the reduced three-dimensional asymmetric instabilities from the use of a symmetry boundary condition at the hole centreline.

More hybrid LES studies on single-hole cooling have been carried out since then, and improvements has been made based on the initial 1-equation DES approach. For example, Foroutan and Yavuzkurt [58] compared the behaviour of a realizable *k-ε* RANS model- with a realizable *k-ε* model-based DES approach. They simulated the 30°-inclined single-hole cooling case measured by Sinha and his colleagues [20] with a fully structured 1.4-million-cell wall-resolving grid. It is worth mentioning that they also introduced a synthetically generated 10% inflow turbulence intensity level using a 2D vortex method. Enhanced mixing was found by using the DES approach, as well as the introduced inflow turbulence, and, therefore, with improved ACE prediction in the far wake region. However, the jet mixing and main stream entrainment phenomenon were so complex in the near-wake region that both methods failed to give reasonable prediction.

A few years later, Chen and Xia utilised a new hybrid RANS-LES model [5] in single-hole cooling cases. They combined the *k-ω* SST model with an implicit LES model using the wall proximity controller, so that the RANS model was only activated in the near-wall boundary region where the flow was mostly laminar. They studied the canonical single-hole case from [20] with an unstructured 10-million-grid mesh. The study confirmed the potential success of hybrid LES in providing high-fidelity numerical prediction in both the flow field and the ACE for single-hole cooling cases. The study also suggested that the coolant jet development, mixing, and entertainment can be changed significantly when the mainstream is highly turbulent (e.g., 20% turbulence intensity in the combustion chamber).

In recent years, Very Large Eddy Simulation (VLES) has caught some researchers' attention. Jin and his colleagues [59] applied VLES to the canonical single-hole test case by Sinha [20] and compared the results to other popular methods (DES and LES). The VLES model was blended with Wilcox's *k-ω* model using a resolution function determined by the cut-off, integral, and Kolmogorov length scales. The DES model that they used was blended with the *k-ω* SST model, while the LES model used a Wall-Adaptive Local Eddy viscosity (WALE) SGS model. Results based on a 2.5-million-cell grid suggested that the VLES model provides encouraging predictions on both the flow structures and ACE. Delayed Kelvin–Helmholtz instability was found in the DES prediction, which has led to the unsatisfactory cooling effectiveness prediction. The authors also concluded that VLES performs better than the LES, but this is mainly because the grid resolution they used was not good enough for the LES to resolve all the scales, especially in the near-wall region.

Researchers are also using the hybrid LES method to study the performance of different cooling hole shapes. However, the study was mostly conducted using commercial software due to the complexity of the hole geometry and difficulties it brought to meshing. Zamiri and his colleagues [60] studied a 35-degree-inclined laid-back fan shape hole using three different models: LES, Scale Adaptive Simulation (SAS), and DES, with a 6-million-node multi-block structured mesh using ANSYS CFX. They concluded that LES is the only model that they found to provide acceptable accuracy in cooling performance. They believed that this was due to the LES model's advantage in resolving more complex flow structures when the coolant jet left the laid-back fan shape hole and was mixed with the mainstream, compared to the simple cylindrical hole geometry.

5.2. Multi-Hole

Andreini and his colleagues at the University of Florence, which is mentioned a few times in the early sections, also explored the application of hybrid LES in a multi-hole effusion cooling case [61–63]. In the work by Mazzei et al. [61], a SST SAS model and a DES model were used to predict the performance of a lean-burn combustor liner effusion cooling with swirling combustion jets. However, effusion jets were not simulated directly owing to the complex geometry of the fuel nozzle and combustor chamber. A constant heat flux boundary condition was applied to the effusion-cooled plate following their previous study on effusion cooled flat plates. To make the simulations comparable to experiments,

the heat mass transfer analogy was retrieved with two extra equations for two passive scalars that track the flow mixing of both the slot and effusion cooling. Two different grid resolutions were used, 8-million and 21-million, but the results were close as only 40% of resolution increase was applied to each direction owing to the unstructured manner of the mesh. The authors concluded that the study revealed the potential of using SAS in simulating the combustor liner effusion cooling with a swirling flow, with a similar or better accuracy to DES under the limited computational cost. In the following study [62], two different effusion models, the adiabatic homogeneous model (AHM) and the source-based effusion model (SAFE), were compared. The former assumes uniform coolant injection on the flat plate, while the latter injects point mass to the main flow. The results suggested that both methods were fine in predicting the momentum exchange between the coolant and mainstream, but the SAFE method provided higher-fidelity results in heat transfer and cooling effectiveness. Lenzi [63] continued the previous study and used a new hybrid LES method named stress-blended eddy simulation (SBES) approach. In his study, the effusion coolant jets were actually modelled using a much finer unstructured mesh of 50-million elements. The study suggested that a few unsteady interactions between the swirling jets and the coolant jets play a crucial role in defining the coolant film capabilities, which cannot be properly reproduced by steady-state methods.

A compound angle effusion cooling arrangement was studied by a research group from France [64]. The experiment carried out by Zhang et al. [65] was simulated by Arroyo and his colleagues using the differential Reynolds stress model (DRSM) in conjunction with a generalized gradient diffusion hypothesis (GGDH) and a hybrid RANS–LES method: zonal detached eddy simulation (ZDES), with CHT effects also being taken into account. The authors proposed a new method to calculate the length scales for the ZDES method. Encouraging results were obtained by both methods, but the authors found that the transition region from RANS to LES in the ZDES needed to be taken extra care. The authors also stated that since the ZDES method is 50% slower than the DRSM method, it is not the preferred method to them for multi-hole effusion cooling.

Chen et al. [5–7] utilised a new hybrid RANS-LES method in predicting the combustor liner effusion cooling. The method used the RANS approach as a wall-model to reduce the near-wall resolution requirement of LES, which is due to increasing the resolution to resolve the compressed and stretched turbulent structures closer to the wall. An 18-million-cell unstructured mesh was generated with a wall-resolving y^+ value. A comparison with URANS results suggested that the hybrid LES approach performed much better in reproducing the coolant jet mixing, separation, and reattachment, and thus providing better prediction in the coolant film formation and surface ACE. Further study with low and high inflow turbulence intensities, which were generated by the synthetic eddy method (SEM), and a comparison with experimental measurements suggested that the highly turbulent flow in the combuster chamber (20% intensity) substantially leads to wider spreading of the coolant film and, thus, requires a higher blow ratio to achieve a similar level of effectiveness in the downstream region.

6. Large-Eddy Simulations

LES has been used to model effusion cooling flows in a diverse range of studies including single- and multi-hole cooling configurations. A snapshot of the turbulent structures and centre-plane velocity field simulated with LES showing its ability to model large-scale turbulent structures and capture the turbulent mixing between the hot mainstream and cold jet is presented to illustrate the LES solution in Figure 10. Within this section, LES modelling approaches and schemes are highlighted alongside their significant contributions and applications. A table of reviewed cases is presented in Table 4.
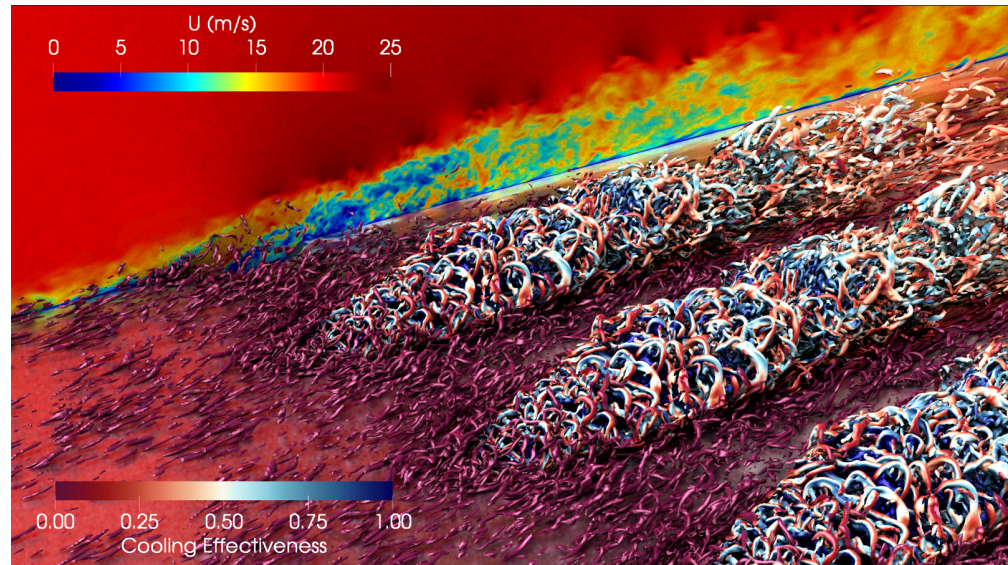
Figure 10. LES solution showing turbulent structures and mixing behaviour of coolant downstream of a single row of cooling holes with an 80-million cell mesh. This figure is an original extension of the earlier work published by Ellis and Xia [10].

Table 4. Table of reviewed LES cases including inflow and sub-grid scale models.

Paper	Year	Sub-Grid Scale Model	Turbulent Inflow Model
Tyagi and Acharya [66]	2003	DMM	No inflow turbulence
Iourokina and Lele [67]	2005	Dynamic Smagorinsky	Recycle-Rescaling [68]
Renze et al. [69,70]	2008	MILES	Recycle-Rescaling
Guo et al. [71]	2006	Implicit	Recycle-Rescaling [68]
Rozati and Tafti [72]	2008	Dynamic Smagorinsky ($Pr_{sgs} = 0.5$)	No inflow turbulence
Bodart et al. [56]	2013	Vreman's eddy viscosity model [73]	Digital filtering [74]
Oliver et al. [75]	2019	WALE	No inflow turbulence
Ellis and Xia [10]	2022	WALE ($Pr_{sgs} = 0.4$)	Digital filtering [76]
Kang et al. [77]	2021	WALE	Turbulence generated by upstream cylinders
Hao and di Mare [78–80]	2023	Implicit	Digital filtering [81]
Mendez et al. [82]	2008	WALE	Periodic (assumes asymptotic effusion behaviour)
Renze et al. [83]	2009	MILES	No inflow turbulence
Motheau et al. [84]	2012	WALE	Synthetic turbulence [85]
Konopka et al. [86]	2013	Standard Smagorinsky	Synthetic turbulence [85] Recycle-Rescaling [87]
Sung et al. [88]	2016	Implicit wall resolved and modelled	No inflow turbulence
Ledezma [49]	2016	WALE	No inflow turbulence

6.1. Single-Hole

Tyagi and Acharya [66] used a Dynamic Mixed Model (DMM), outlined by Moin et al. [89] and Vreman et al. [90], to model the subgrid-scale stress tensor and scalar flux vector. This was used to model the cooling flow of an inclined cylindrical jet at blowing ratios of 0.5 and 1.0 for a density ratio of 1.0. An explicit second-order accurate Adams–Bashforth scheme was used to discretise the equations in time, while a third-order upwind-difference scheme was used for convective schemes, and the remaining schemes were discretised with a fourth-order central differencing scheme. The results showed that the time-averaged velocity profiles provided reasonable agreement with measured data of Lavrich and Chiapetta [91]

for both BR conditions. The ACE results were compared against the experimental data of Sinha et al. [20], although differences were present in the density ratio. The centreline cooling effectiveness at $BR = 0.5$ matched the experimental data [20], with small differences close to the coolant hole.

Parallel interface coupling between a compressible and low-Mach-number computational code was pursued by Iourokina and Lele [67] for predicting film cooling performance across turbine leading edges. The coupling enabled the low-Mach-number code to model the plenum chamber, while the compressible code resolved the external flow. Qualitative results were presented for a jet-in-cross-flow to demonstrate the method. This was extended to a single cooling hole [92] with the rescaling-recycling technique of Lund et al. [68] to generate the upstream turbulent boundary layer. A qualitative comparison was presented to the contours published by Pietrzyk et al. [52,53], which showed some agreement, but clear quantitative comparisons could not be made. Later work [93], featuring cooling effectiveness comparisons to Sinha et al. [20], showed comparable centreline effectiveness results aft the cooling hole.

The Monotonically Integrated LES (MILES) technique of Fureby and Grinstein [94] was used by Renze et al. [69,70] for LES studies of a single row of cooling holes. The solved equations were discredited with a mixed central-upwind AUSM scheme with a centred 5-point low-dissipation stencil. The inlet flow was established with a compressible recycling-rescaling method to capture the upstream turbulent flow. The results showed accurate agreement to the velocity data in the experimental results of Jessen et al. [95]. The cooling predictions for $BR = 0.43$ compared well to the experimental results of Sinha et al. [20] at $BR = 0.5$. The results of Sinha et al. [20] showed large differences in lateral coolant spread for varying DR and, thus, the lateral spread cannot be compared between the two cases. The authors showed a strong interaction between the approaching turbulent boundary layer and the effusing jet flow with λ_2 contours, where the upstream turbulent boundary layer was captured with a precursor recycling-rescaling simulation.

Guo et al. [71] investigated a 90° and a 30° inclined single-hole cooling geometry for low blowing ratios of 0.1 and 0.48. The LES was performed with the Navier–Stokes equations for compressible flow discretised with a mixed central-upwind AUSM scheme with low numerical dissipation. For the turbulent inflow, the rescaling-recycling method of Lund et al. [68] was used. The LES results showed the formation of the counter-rotating vortex pair, separated flow, and the complex anisotropic state of the turbulence characteristics shown with the invariant technique.

An investigation of the blowing ratio on cooling holes distributed across turbine blade leading edges was conducted by Rozati and Tafti [72] using LES. The LES was performed on a non-dimensional form of the incompressible Navier–Stokes equations where the subgrid-scale stresses were modelled with a dynamic Smagorinsky model. The subgrid-scale turbulent heat flux was modelled using a subgrid-scale Prandtl number of 0.5. Blowing ratios of 0.4, 0.8, and 1.2 were studied, showing that at higher blowing ratios, the coolant-mainstream mixing was greater, and thus, the cooling effectiveness on the turbine blade was reduced.

High-fidelity LES was performed by Bodart et al. [56] on an inclined jet with results showing the jet structure and the discrepancies of the GDH model. A grid of 52 million cells was used to spatially resolve turbulent structures. Structured block meshing was employed within regions of interest, and unstructured cells were applied to coarsen the mesh at the upper wall. Sub-grid scale stresses were modelled with Vremen's eddy viscosity model [73]. At the inlet boundary condition, the synthetic turbulence method of Xie and Castro [74] based upon the digital filtering method of Klein et al. [96] was used to generate physical upstream turbulent flow. The turbulent inflow was in agreement with the mean velocity profile and Reynolds stresses found in the PIV experiment by Coletti et al. [47]. The investigation showed that the normal and spanwise components of turbulent scalar flux opposed the gradients, as modelled by the GDH. However, the streamwise component did not oppose the gradient and deviated from the closure.

Shaped film cooling holes were investigated with LES by Oliver et al. [75] to understand the role of Mach number in cooling performance. The LES used a finite difference approach on overset methods with the compressible Navier–Stokes equations discretised with a sixth-order Padé method and a 4th-order Runge-Kutta method. The grids used consisted of 42.5 million grid points, and the subgrid-scale stresses were modelled with the WALE model. The laterally averaged and lateral maximum cooling results were in agreement with the presented experimental data for a mainstream Mach number of 0.25. At a Mach number of 0.5, the cooling effectiveness performance decreased, and the time-averaged coolant distribution exhibited a lateral skewness, and the temporal data showed bimodal stability, which was not present in the low Mach number case.

Ellis and Xia [10] investigated the impact of mainstream freestream turbulence in LES of a single row of film cooling holes. No inflow turbulence, near-wall turbulent boundary layer, and freestream turbulence inflow at 20% intensity were investigated. The inflow turbulence was generated with the digital filtering method, originally used for urban flows [76]. The WALE model was used to model the subgrid-scale stresses, while the convective schemes were discretised with a central-upwind blended scheme to capture the fine-scale turbulent structures in the cooling jet. The subgrid-scale turbulent heat flux was modelled using a subgrid-scale Prandtl number of 0.4. Turbulent structures showed interactions between the upstream turbulence and the cooling jet, as shown in Figure 11. The interactions showed increasing contributions to the lateral spreading of the coolant from the no-inflow case to the turbulent boundary layer case and to the freestream turbulence case. The replication of the experimental results, where a turbulent boundary layer was measured upstream of the cooling hole, was only achieved with the turbulent boundary layer case. This demonstrates the importance of modelling the upstream turbulence in these cooling flows.
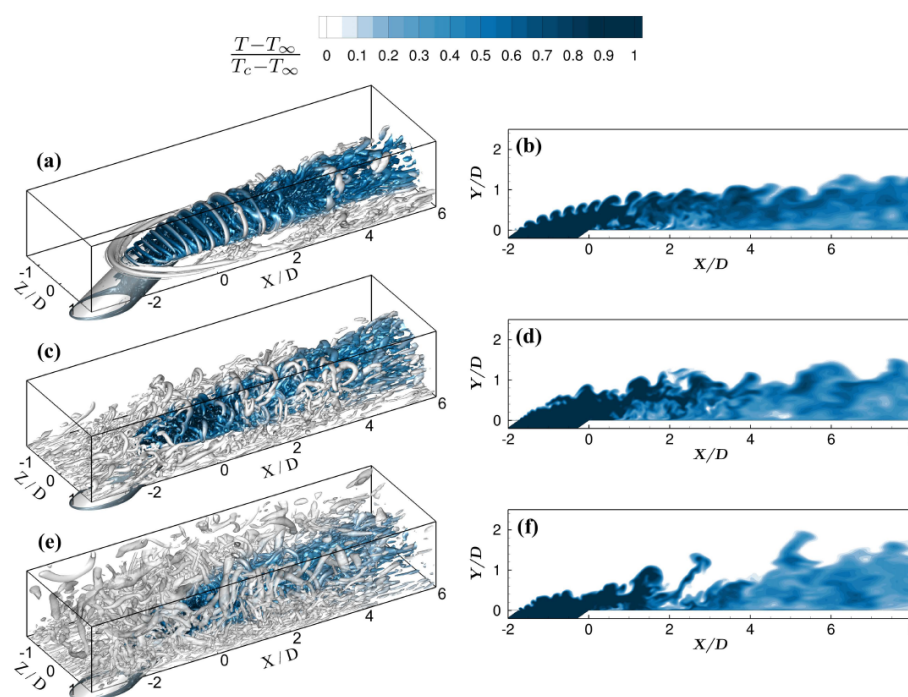

Figure 11. Visualisation of large scale turbulent structures with λ_2 and normalised temperature for a case with no inflow turbulence (**a**,**b**), near-wall turbulent boundary layer (**c**,**d**) and freestream turbulence (**e**,**f**). Reprinted from Int. J. Heat Mass Trans., Vol. 195, Ellis and Xia [10], Impact of inflow turbulence on large-eddy simulation of film cooling flows, published by Elsevier, under the terms of the CC BY 4.0 license.

Kang et al. [77] used LES to investigate the impact of upstream freestream turbulence by introducing upstream geometrical cylinder into the simulation of a single row of fan-shaped cooling holes to mimic the high turbulence intensity found in combustor flows. The simulations were conducted at blowing ratios of 1.0 and 2.0 for a density ratio of 2.0. The diameter of the cylinders was modified to deliver a turbulence intensity of 13% to the cooling holes. ANSYS CFX, a commercial CFD package, was used by the authors using a WALE model for the subgrid-scale stresses. The introduction of the upstream cylinders showed a large decrease in downstream centreline effectiveness for a blowing ratio of 2.0.

Hao and di Mare [78–80] conducted a series of LES simulations of single cylindrical and fan-shaped cooling holes. An in-house code used an implicit LES finite volume approach, solving the Navier–Stokes equations with viscous fluxes discretised with a centred second-order accurate scheme and inviscid fluxes evaluated with a Roe–Riemann solver with a biased three-point stencil that provides third-order accuracy away from discontinuities. Hao and di Mare [78] showed good agreements with the experimental surface cooling effectiveness, and the velocity profiles exhibited correct trends with minor differences closer to the cooling hole. The article identifies that the turbulence properties of coolant jets do not achieve self-similar behaviour when scaled with traditional local velocity defects and jet-layer thickness but identifies a suitable scaling method for the presented cases.

6.2. Multi-Hole

Mean velocity and velocity fluctuations over an infinite multi-perforated plate were compared in the LES of Mendez et al. [82]. Periodicity was used across the computational domain with freestream-type boundary conditions used to force the appropriate mean vertical flow rate with a source term to ensure that the infinite multi-perforated plate flow was sustained. Comparisons with experimental data showed that the finest mesh explored captured the mean velocity trends but over-predicted the value; however, the free shear layer of the cooling hole was shown to be in good agreement with the experiment.

Renze et al. [83] presented LES results from a geometry featuring three staggered rows of fan-shaped cooling holes. The numerical methodology is consistent with previously published work [69,70]. The cooling holes were separated laterally by a pitch of 3D and a spanwise spacing of 6D. The results showed a difference in mixing behaviour in successive rows where the turbulent kinetic energy was highest ahead of the first row with declining turbulence production in the following rows. Cooling effectiveness was improved after each row with the decay of cooling effectiveness reduced after each row. In the later part of the article, the turbulent Prandtl number was derived using the resolved wall-normal eddy viscosity and diffusivity, showing a range of values from 0.4–2.5.

Motheau et al. [84] investigated a multi-perforated plate with elliptical-shaped inlet and exit hole sections that mimicked the laser drilling technique used for effusion cooling holes. The holes were positioned in a staggered arrangement with longitudinal spacing and pitch between holes that replicated an experimental combustor. LES was performed using the Advanced Virtual Burner Project (AVBP) code developed at CERFACS and IFP (see Wolf et al. [97]). Discretisation in space and time was performed with a third-order Taylor–Galerkin-type scheme. Two subgrid-scale models were investigated: a standard Smagorinsky model and the WALE model. A previous study of the same geometry found that 10 million tetrahedral cells were sufficient to reproduce the core features of the flow [82]. Motheau et al. [84] showed that the WALE model with synthetic turbulence injection provided the best comparison to the experiments. Ultimately, the LES was used to demonstrate the impact of combustion instability on the cooling performance. It was found that acoustic forcing in the combustion chamber limits the coolant mass flow rate through the effusion cooling holes.

A multi-hole fan-shaped cooling geometry with an adverse pressure gradient was investigated with LES by Konopka et al. [86]. The rescaling-recylcing technique of El-Askary et al. [87] was used to generate realistic inflow turbulence. The pressure gradient was achieved by manipulating the pressure and streamwise velocity distribution on the up-

per boundary. The results were in close agreement with the LES results of Renze et al. [83] and showed that the mild adverse pressure gradient did not impact wall cooling effectiveness distribution, in agreement with Hay et al. [98]. In the boundary layer, the mild adverse pressure gradient thickened the thermal boundary layer, and inspections of the turbulent heat flux showed increased magnitudes in the mid and upper regions of the jet shear flow.

Sung et al. [88] presented a detailed LES simulation resolving 52 cooling holes across an eight-row multi-hole effusion cooling array. The simulation used the low-Mach pressure projection solver detailed in Ham [99]. Two blowing ratios were investigated covering an attached coolant case ($BR - 0.457$) and a detached coolant case ($BR = 1.22$). Wall-resolved and wall-modelled LES were compared, where the meshes were composed of 530 million and 290 million cells, respectively, using a tetrahedral mesh with prism layers at the wall. The detached case showed very similar behaviour between the two approaches across each row. For the attached case, the laterally-averaged cooling differed between the two approaches for the first three rows of cooling holes, but both methods overpredicted the experiment in this region but provided good agreement for the downstream region.

Effusion cooling was studied with LES by Ledezma [49] using a 47-million- and 18-million-cell hexadominant unstructured mesh across 8 rows of staggered cylindrical cooling holes. The authors used the SIMPLEC solver in Fluent v14.5, using a bounded second-order central differencing scheme for spatial terms and a second-order backward time stepping scheme. Subgrid scale stresses were modelled with the WALE model. The results of the fine mesh were in close agreement with the experiment's laterally-averaged cooling measurements and presented lateral distributions for blowing ratios of 0.6, 0.8, and 1.0.

7. Machine Learning Augmented Modelling

Machine learning has been used in a variety of strategies to improve the modelling of effusion cooling flows or directly complete the modelling. In turbulence modelling, machine learning techniques have provided improvements that have attempted to tackle the stagnated development seen at the start of the 21st century [100]. Machine learning and data-driven methods have taken advantage of the dense high-fidelity numerical and experimental datasets, coupled with physical insights into the flow. For effusion cooling flows, machine learning-augmented modelling has been employed to improve the poor predictions that RANS simulations provide, as shown in Section 4. Within this section, machine learning augmented modelling techniques used for effusion cooling flows through single-hole and multi-hole studies are reviewed.

Jet-in-crossflow configurations were investigated by Ling et al. [101], where data-driven methods were used to improve the anisotropic turbulent predictions of the k-ε turbulence model in an *a posteriori* analysis. A random forests algorithm was trained using a basis of 49 invariant, non-dimensional input features constructed from the flow's mean velocity, the mean velocity gradients, the turbulent kinetic energy and dissipation rate, the density, the pressure gradients, and the molecular and turbulent viscosities. The model output barycentric coordinates associated with Reynolds anisotropy eigenvalues. This permitted a prediction of the anisotropy that ensured realizability by constraining their values to well-defined limits. The generalisation of the model was assessed by applying it to a wavy wall case and flow over a square cylinder.

Milani et al. [102] used machine learning to improve the turbulent heat flux closure in RANS simulations. A supervised machine learning algorithm was applied to infer a turbulent diffusivity field for the GDH based on the turbulent diffusivity calculated from a high-fidelity LES or DNS simulation. A skewed jet-in-cross-flow and a wall-mounted cube in cross-flow were used to train a random forest algorithm, and the model was then tested on an inclined jet-in-cross-flow. Contours of turbulent diffusivity showed improved results compared to the LES-described values. A forward propagation step to investigate the ACE, which is the ultimate goal, produced results similar to the LES ACE distribution. Later studies by Milani et al. [103] used the same approach and demonstrated

the *a priori* performance of a favourable pressure gradient film cooling hole flow. Rather than LES or DNS data, extensive high-resolution experimental datasets were employed in this case. Using the random forest model for turbulent diffusivity, the injection region showed reduced error of the mean scalar field; however, the wall showed an increase in the error. The use of this approach showed some degree of improvement and illustrated a potential method for improving RANS turbulent closures.

Interpreting complex machine learning models was the subject of the later study of Milani et al. [103] using a feature analysis technique. Rule extraction from the random forest trees identified the wall distance and eddy viscosity as critical features in the model. Pointwise feature usage, describing a point-by-point analysis of the features used in the algorithm, showed that certain features were only critical in localised regions. For example, the eddy viscosity is less significant in determining the turbulent diffusivity near the wall but becomes more important within the freestream. A sixth-order term in the velocity gradient becomes very prominent below the core of the jet where it is known that a constant turbulent Prandtl number overestimates the wall-normal transport. These techniques remove the "black box" and opaque nature of the machine learning algorithms while providing modelling insights that can be incorporated into further studies.

The generalisation of machine learning models of turbulent diffusivity using a non-uniform turbulent Prandtl number was investigated by Milani et al. [104]. Results from the machine-learnt turbulent diffusivity model were observed to generalise well to a blowing ratio of 1.0 when the model was trained upon different datasets. However, it did not generalise well to the higher blowing ratio case. Two dimensionality reduction techniques, Principal Component Analysis (PCA) and t-distributed Stochastic Neighbour Embedding (t-SNE), were used to identify regions in which the datasets deviated from each other. This analysis showed that the data from the higher-blowing ratio case were a superset of those from the lower-blowing ratio case. The results highlighted that effective models must incorporate datasets spanning different operating conditions for the configuration of interest. It was highlighted that this approach lacked sufficient anisotropy in the turbulent heat flux, and the results reported did not incorporate a non-linear anisotropic Reynolds stress field.

A later work by Ellis et al. [8] investigated the use of shallow neural networks and random forest algorithms to inform a function for the HOGGDH coefficient for single-row inclined cylindrical cooling holes with a k-ω SST model. The HOGGDH model was employed due to its improved modelled turbulent heat flux vector direction observed in the study of a heated blunt plate flow [9]. The models were trained on two LES single-hole cylindrical cases and tested on a third case not seen in the models' training. The shallow neural network and random forest models were able to reconstruct an LES-derived HOGGDH coefficient that accurately reproduced the turbulent heat flux magnitude. However, the form of the HOGGDH showed discrepancies in the turbulent heat flux direction and components in the downstream region of the jet. When the model was employed in a RANS solver, the model improved predictions over a standard GDH approach, but only minor improvements were seen over a HOGGDH model with a constant coefficient of 0.6.

Ellis and Xia [11] implemented a Tensor Basis Neural Network (TBNN) model (Figure 12) of turbulence anisotropy trained on high-fidelity LES data using 10 tensor features and 17 scalar features. The model and its implementation in RANS showed improved *a posteriori* results. When combined with a standard HOGGDH model (with $c_\theta = 0.6$), the results showed improved predictions of lateral coolant distributions, but the results in the initial region of jet development were best predicted when combined with the GDH model. The model was then used in a RANS simulation of a multi-row effusion cooling flow, which was experimentally investigated by Andrei et al. [48]. Spanwise-averaged cooling performance (provided in Figure 13) was improved using a combination of the TBNN turbulence anisotropy model and the HOGGDH turbulent heat flux closure. The contours provided in the article showed a qualitative improvement in the lateral coolant spread in agreement with the experimental contours.
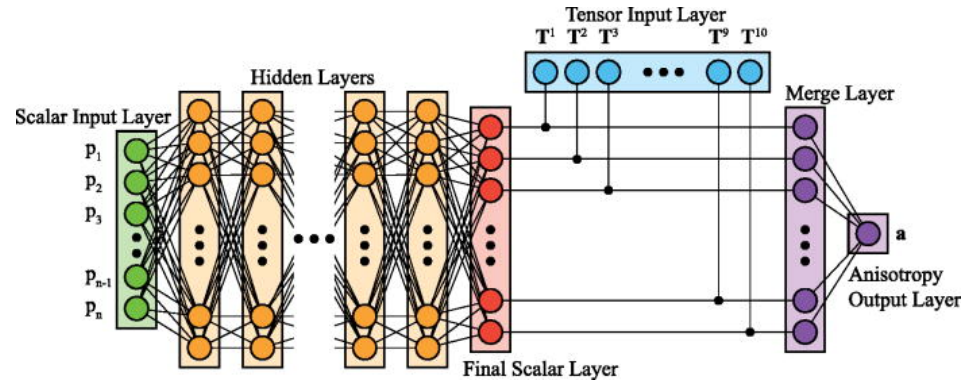
Figure 12. Tensor-basis neural network (TBNN) model used by Milani et al. [105] and Ellis and Xia [11,106] for turbulent diffusivity tensors and turbulence anisotropy, respectively. Reprinted from Phys. Fluids, 35, Ellis and Xia [11], Data-driven turbulence anisotropy in film and effusion cooling flows, published by AIP Publishing, under the terms of the CC BY 4.0 license.

Milani et al. [105] implemented the TBNN architecture (Figure 12) to further improve turbulent scalar flux predictions by introducing anisotropy into the turbulent scalar flux vector and addressing the counter gradient transport. Two key types of counter-gradient transport were highlighted: cross-gradient transport in the windward shear layer and non-local effects in the near-wall region aft the coolant injection. In contrast to the machine-learnt turbulent diffusivity of Milani et al. [102,104], the TBNN architecture learns a turbulent diffusivity tensor, D_{ij}, included in the Reynolds-averaged scalar transport equation (Equation (5)). The results showed a qualitative improvement across the centreline planes; however, the spanwise planes showed smaller improvements. Within the work, the issue of numerical stability for tensor-based diffusivity was addressed. The tensor was forced to be positive semi-definite to satisfy the stability within the diffusion–convection equation, which deviated from the machine-learnt term.
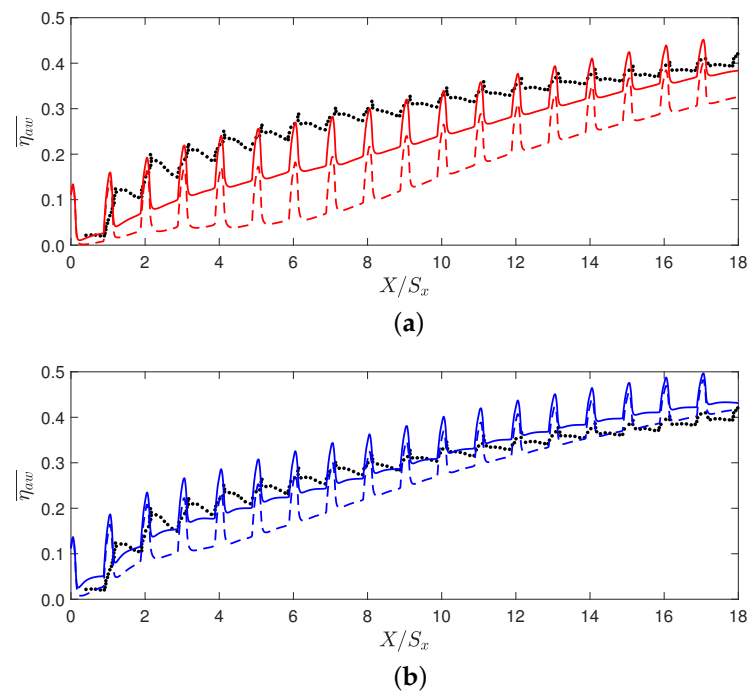

(a)

(b)

Figure 13. Spanwise averaged ACE for the multi-hole cooling array case compared to experimental datasets [48] [•]. Reprinted from Phys. Fluids, 35, Ellis and Xia [11], Data-driven turbulence anisotropy in film and effusion cooling flows, published by AIP Publishing, under the terms of the CC BY 4.0 license. (**a**) Experimental dataset [•], *SST-GDH* [-·-] and *TBNN-SST-GDH* [——]. (**b**) Experimental dataset [•], *SST-HOG* [- - -] and *TBNN-SST-HOG* [——].

$$\frac{\partial}{\partial x_i}(\overline{u}_i\overline{c}) = \frac{\partial}{\partial x_i}\left(\frac{\nu}{Sc}\frac{\partial\overline{c}}{\partial x_i}\right) + \frac{\partial}{\partial x_i}\left(D_{ij}\frac{\partial\overline{c}}{\partial x_j}\right) \tag{5}$$

Milani et al. [107] addressed the question of machine learning model generality. The generality question refers to the ability of a model to perform on different flows that it was not trained upon. The turbulent nature of each flow is different, and it is well known that turbulence models behave differently across a broad range of flows. Milani et al. [107] showed that models trained and tested on the same class of flow produce significant improvements to the mean scalar field when the TBNN model from Milani et al. [105] is used. When trained and tested on different classes of flows, the model does not improve the results but merely replicates the baseline. This shows that, although this approach is not able to generalise, it does not produce non-physical results.

Recent work by Ellis and Xia [106] combined a TBNN (Figure 12) turbulence anisotropy model [11] with the published spatially varying HOGGDH coefficient model [8] and a *k*-*ω* SST model. The study investigated single-hole inclined cylindrical cooling holes. Although surface cooling effectiveness distributions only showed marginal improvements over the standard *k*-*ω* SST model with baseline HOGGDH, large improvements to the temperature profiles through the coolant jet were observed with improved mean velocity and turbulent profile predictions. The authors concluded their article by identifying that the approach still under-predicted the turbulent kinetic energy field and further machine learning models could be extended to improve the turbulent model transport equations.

Deep neural networks were used by Wang et al. [108] to directly predict solid temperatures and stresses in multi-hole cooling arrangements using CFD with solid conductive heat transfer. The simulations were conducted with ANSYS Fluent using the Realizable k-epsilon model. Latin Hypercube Sampling (LHS) was used to support the training dataset generation. The deep neural network used inputs such as blowing ratio, density ratio, inclination angle, hole pitch, and spacing. The results showed that the deep neural network was able to reproduce the CFD results for cases not seen with a mean absolute percent error of 0.5% and 0.08% for temperature and stresses, respectively. The authors reported that the approach was only valid within the scope of parameters studied, and the method would not be suitable for cases that significantly differ from the training dataset. In addition, these approaches are only as ideal as the CFD used to train the model.

Yang et al. [109] investigated the use of a Convolution Neural Network (CNN) to quantify the cooling superposition in novel multi-hole cooling arrays. CFD simulations of 13 multi-hole cooling cases were used to train and test the model. The input to the CNN model was a binary input matrix where a 1 defines the spatial location of a cooling hole while the model output is the surface cooling effectiveness distributions. The model then predicts the cooling performance of novel and unseen hole distributions. A later work by Yu et al. [110] implemented a transfer learning method designed to assimilate both numerical and experimental data for effusion cooling. The model trained was able to predict the performance of random cooling hole configurations that would provide a useful rapid design tool.

A low-cost, novel approach for simulation effusion cooling walls in a combustor sector was introduced by Paccati et al. [111]. The geometry of the effusion cooling holes was replaced with two-dimensional boundary source terms for the effusion hole velocity and turbulence terms that are modelled with a combined reduced-order and regression approach to form the surrogate model. The model was trained with the RANS CFD of a single cooling hole, providing accurate predictions over an array of operating conditions. Good agreement was found in the velocity profiles between a pure CFD solution of the combustor sector with resolved effusion cooling holes and when the source term surrogate model was used, but cooling predictions across the effusion cooling plate showed over-predictions at the cooling hole trailing edge.

Physics-Informed Neural Networks (PINNs) were investigated by Huang et al. [112,113]. The method provides a meshless approach to resolving inverse problems in fluid mechanics and other fields. Huan et al. [112] used PINNs to reconstruct the time-averaged field of a complex jet-in-crossflow case using a tensor-based eddy viscosity to improve the prediction of anisotropy that jet flows feature. With limited observations, the authors found that the approach provided some success in replicating the time-averaged field compared to when using a scalar eddy viscosity.

In a later work, Huang et al [113] used PINNs to reconstruct the three-dimensional flow field of a swirling combustor flow with an effusion cooling plate from two-dimensional two-component data. The PINN was formulated using mean values of velocity, pressure, and passive scalar as well as the Reynolds stress tensor and turbulent passive scalar flux. Losses were shown to be a summation of a weighted loss from the Partial Differential Equation (PDE) losses and the observational (experimental) loss, but boundary condition losses were not shown in the final loss metric. The results found some success when data were trained on just the two-dimensional two-component data, but the authors found significant improvements when observational data of the coolant passive scalar, measured with pressure-sensitive paint (PSP), were also included. The authors highlighted that the method requires large volumes of data and should only supplement three-dimensional modelling, but a future work that helps capture complex turbulent wall-bounded flows could improve the approach.

Despite the impressive efforts of machine learning to improve effusion cooling prediction, a couple of key questions remain to be addressed in the near future. Firstly, the choice of input features between primary physical variables and high-order tensors can be less straightforward to determine. Using primary physical flow properties can be more physics-informing while high-order tensors can be more numerically unstable, making them less attractive in practice. Secondly, the "black box" nature of some models reduces the traceability and can prohibit their adoption by industry. Finally, error estimation is still a major topic among machine learning and data-driven algorithm developers. Ultimately, one ought to have the knowledge of what the potential error bounds are before applying such machine learning-augmented models.

8. Concluding Remarks and Outlook

With the advancement of computing power over the past few decades, we have witnessed numerical simulation and modelling as a methodology for studying effusion cooling phenomena on a general trend towards higher-fidelity, more resolved, and better predicted solutions. And yet, the demand for even higher accuracies of cooling predictions and better understanding of effusion mechanisms appears to grow even faster in order to satisfy the engineering needs. Based on our extensive review of computational works over the recent years, a few observational notes can be made:

- First-order principles and conservation law-based control volume methods are still relevant today. However, their practical usage is seen to have reduced, mainly due to the lower likelihood of canonical geometries and simplified boundary conditions.
- For the RANS, however, there have been an overwhelming body of work producing reasonable results. RANS models tend to predict an elongation of coolant track in the streamwise direction while under-predicting the cooling jet's lateral spreading. Mismatches of ACE distributions can be easily found in comparison studies against measurements, despite their superior computational efficiency to their higher-fidelity counterparts.
- Not surprisingly, eddy-resolving methods, which include LES and hybrid RANS-LES, have seen great increases in their application in practice, offering more accurate accounts for longitudinal and lateral distributions of ACE and surface temperature prediction. More importantly, they also come with the resolved Reynolds stresses and turbulent heat fluxes for interrogation that may reveal more underlying flow physics. However, these are at significant computational costs as our listed works have shown.

In modern cooling designs, given the effectiveness strongly relies on the shape of the cooling holes, it would be impossible for eddy-resolving methods alone to provide all the answers to the vast varieties of design questions, leading to the next bullet point.

- The power of machine learning algorithms cannot be underestimated as they have demonstrated their huge potential to exploit the "big data" created by previously mentioned eddy-resolving methods. The physics-based input to the TBNN framework, for example, was shown to produce encouraging results.

Looking forward, it is foreseeable that eddy-resolving methods will continue to develop and evolve with cost reduction in mind, especially with the likes of wall-modelled LES and hybrid RANS-LES. On the other hand, the future of RANS models, owing to their simplicity and low-cost nature, with machine learning-aided data-driven augmentation beyond the limits of conventional eddy viscosity and GDH hypotheses looks particularly bright.

Abbreviations

The following abbreviations are used in this manuscript:

ACE	Adiabatic cooling effectiveness
AHM	Adiabatic homogeneous model
AI	Artificial intelligence
ANN	Artificial neuron network
AVBP	Advanced virtual burner project
CFD	Computational fluid dynamics
CHT	Conjugate heat transfer
CNN	Convolution neural network
DDES	Delayed detached-eddy simulation
DES	Detached-eddy simulation
DMM	Dynamic mixed model
DNS	Direct numerical simulation
DRSM	Differential Reynolds stress model
GGDH	Generalized gradient diffusion hypothesis
HOGGDH	Higher-order generalised gradient diffusion hypothesis
LES	Large-eddy simulation
LHS	Latin hypercube sampling
MILES	Monotonically integrated LES
ML	Machine learning
MRC	Magnetic resonance concentration
PCA	Principal component analysis
RANS	Reynolds-averaged Navier–Stokes
SAFE	Source-based effusion model
SBES	Stress-blended eddy simulation
SGS	Sub-grid scale model
RNG	Re-Normalisation Group
RSM	Reynolds stress model
SAS	Scale Adaptive Simulation

SEM	Synthetic eddy method
SST	Shear stress transport model
TBNN	Tensor basis neural network
VLES	Very large eddy simulation
WALE	Wall-adaptive local eddy viscosity
GDH	Gradient diffusion hypothesis
ZDES	Zonal Detached-eddy simulation

References

1. Goldstein, R.J. Film cooling. *Adv. Heat Transf.* **1971**, *7*, 321–379.
2. Wang, W.; Yan, Y.; Zhou, Y.; Cui, J. Review of Advanced Effusive Cooling for Gas Turbine Blades. *Energies* **2022**, *15*, 8568. [CrossRef]
3. Aumeier, T.; Behrendt, T. Application of an Aerothermal Model for Effusion Cooling Systems and Finite Rate Chemistry in Aero-Engine Combustors. In Proceedings of the THMT15—8th International Symposium On Turbulence Heat and Mass Transfer, Sarajevo, Bosnia and Herzegovina, 15–18 September 2015. [CrossRef]
4. Fric, T.F.; Roshko, A. Vortical structure in the wake of a transverse jet. *J. Fluid Mech.* **1994**, *279*, 1–47. [CrossRef]
5. Chen, X. A Hybrid LES-RANS Approach for Effusion Cooling Prediction. Ph.D. Thesis, Loughborough University, Loughborough, UK, 2018.
6. Chen, X.; Xia, H. Hybrid LES-RANS study of an effusion cooling array with circular holes. *Int. J. Heat Fluid Flow* **2019**, *77*, 171–185. [CrossRef]
7. Chen, X.; Krawciw, J.; Xia, H.; Denman, P.; Bonham, C.; Carrotte, J. Study of an effusion-cooled plate with high level of upstream fluctuation. *Appl. Therm. Eng.* **2021**, *184*, 116126. [CrossRef]
8. Ellis, C.D.; Xia, H.; Page, G.J. LES informed data-driven modelling of a spatially varying turbulent diffusivity coefficient in film cooling flows. In *Turbo Expo: Power for Land, Sea, and Air, Proceedings of the ASME Turbo Expo 2020: Turbomachinery Technical Conference and Exposition, Virtual, 21–25 September 2020*; American Society of Mechanical Engineers: New York, NY, USA, 2020; Volume 84171, p. V07BT12A029.
9. Ellis, C.D.; Xia, H. Turbulent closure analysis in heated separated and reattached flow using eddy-resolving data. *Phys. Fluids* **2020**, *32*, 045115. [CrossRef]
10. Ellis, C.; Xia, H. Impact of inflow turbulence on large-eddy simulation of film cooling flows. *Int. J. Heat Mass Transf.* **2022**, *195*, 123172. [CrossRef]
11. Ellis, C.D.; Xia, H. Data-driven turbulence anisotropy in film and effusion cooling flows. *Phys. Fluids* **2023**, *35*, 105114. [CrossRef]
12. Wilcox, D. *Turbulence Modeling for CFD*; Number v. 1 in Turbulence Modeling for CFD; DCW Industries: La Cañada, CA, USA, 2006.
13. Choi, H.; Moin, P. Grid-point requirements for large eddy simulation: Chapman's estimates revisited. *Phys. Fluids* **2012**, *24*, 011702. [CrossRef]
14. Davidson, P. *Turbulence: An Introduction for Scientists and Engineers*; Oxford University Press: Oxford, UK, 2015.
15. Spalart, P. Detached-Eddy Simulation. *Annu. Rev. Fluid Mech.* **2009**, *41*, 181–202. [CrossRef]
16. Baldauf, S.; Schulz, A.; Wittig, S.; Scheurlen, M. An overall correlation of film cooling effectiveness from one row of holes. In Proceedings of the ASME 1997 International Gas Turbine and Aeroengine Congress and Exhibition, Orlando, FL, USA, 2–5 June 1997; American Society of Mechanical Engineers: New York, NY, USA, 1997; p. V003T09A010.
17. Le Grives, E. Vorticity Associated with the Penetration of a Jet into a Cross Flow. *J. Eng. Power JULY* **1978**, *100*, 465. [CrossRef]
18. Le Grives, E. *Cooling Techniques for Modern Gas Turbines*; Japikse, D., Ed.; Chapter 4 in Topics in Turbomachinery Technology; Concepts ETI, Inc.: Norwich, VT, USA, 1986.
19. Keffer, J.F.; Baines, W.D. The round turbulent jet in a cross-wind. *J. Fluid Mech.* **1963**, *15*, 481–496. [CrossRef]
20. Sinha, A.K.; Bogard, D.G.; Crawford, M.E. Film-cooling effectiveness downstream of a single row of holes with variable density ratio. *J. Turbomach.* **1991**, *113*, 442–449. [CrossRef]
21. Sasaki, M.; Takahara, K.; Kumagai, T.; Hamano, M. Film Cooling Effectiveness for Injection from Multirow Holes. *J. Eng. Power* **1979**, *101*, 101–108. [CrossRef]
22. Sellers, J.P. Gaseous film cooling with multiple injection stations. *AIAA J.* **1963**, *1*, 2154–2156. [CrossRef]
23. Mayle, R.E.; Camarata, F.J. Multihole Cooling Film Effectiveness and Heat Transfer. *J. Heat Transf.* **1975**, *97*, 534–538. [CrossRef]
24. Eckert, E.R.G. Analysis of Film Cooling and Full-Coverage Film Cooling of Gas Turbine Blades. *J. Eng. Gas Turbines Power* **1984**, *106*, 206–213. [CrossRef]
25. Arcangeli, L.; Facchini, B.; Surace, M.; Tarchi, L. Correlative Analysis of Effusion Cooling Systems. *J. Turbomach.* **2008**, *130*, 011016. [CrossRef]
26. Crawford, M.E.; Kays, W.M.; Moffat, R.J. Full-Coverage Film Cooling—Part I: Comparison of Heat Transfer Data for Three Injection Angles. *J. Eng. Power* **1980**, *102*, 1000–1005. [CrossRef]
27. Crawford, M.E.; Kays, W.M.; Moffat, R.J. Full-Coverage Film Cooling—Part II: Heat Transfer Data and Numerical Simulation. *J. Eng. Power* **1980**, *102*, 1006–1012. [CrossRef]

28. Andreini, A.; Facchini, B.; Picchi, A.; Tarchi, L.; Turrini, F. Experimental and Theoretical Investigation of Thermal Effectiveness in Multi-Perforated Plates for Combustor Liner Effusion Cooling. In Proceedings of the Turbo Expo: Power for Land, Sea, and Air, San Antonio, TX, USA, 3–7 June 2013; Volume 3C: Heat Transfer. [CrossRef]

29. Andreini, A.; Da Soghe, R.; Facchini, B.; Mazzei, L.; Colantuoni, S.; Turrini, F. Local Source Based CFD Modeling of Effusion Cooling Holes: Validation and Application to an Actual Combustor Test Case. *J. Eng. Gas Turbines Power* **2014**, *136*, 011506. [CrossRef]

30. Bergeles, G.; Gosman, A.D.; Launder, B.E.; Bergeles, G. The turbulent jet in a cross stream at low injection rates: A three-dimensional numerical treatment. *Numer. Heat Transf.* **1978**, *1*, 217–242. [CrossRef]

31. Leylek, J.; Zerkle, R. Discrete-jet film cooling: A comparison of computational results with experiments. In *Turbo Expo: Power for Land, Sea, and Air, Proceedings of the ASME 1993 International Gas Turbine and Aeroengine Congress and Exposition, Cincinnati, OH, USA, 24–27 May 1993*; American Society of Mechanical Engineers: New York, NY, USA, 1993; Volume 78903, p. V03AT15A058.

32. Walters, D.K.; Leylek, J.H. A Systematic Computational Methodology Applied to a Three Dimensional Film-Cooling Flowfield. In Proceedings of the ASME 1996 International Gas Turbine and Aeroengine Congress and Exhibition, Birmingham, UK, 10–13 June 1996.

33. Walters, D.K.; Leylek, J.H. A detailed analysis of film-cooling physics Part 1: Streamwise injection with cylindrical holes. In Proceedings of the ASME 1997 International Gas Turbine and Aeroengine Congress and Exhibition, Orlando, FL, USA, 2–5 June 1997.

34. Ferguson, J.D.; Walters, D.K.; Leylek, J.H. Performance of turbulence models and near-wall treatments in discrete jet film cooling simulations. In *Turbo Expo: Power for Land, Sea, and Air, Proceedings of the ASME 1998 International Gas Turbine and Aeroengine Congress and Exhibition, Stockholm, Sweden, 2–5 June 1998*; American Society of Mechanical Engineers: New York, NY, USA, 1998; Volume 78651, p. V004T09A077.

35. Hoda, A.; Acharya, S. Predictions of a Film Coolant Jet in Crossflow With Different Turbulence Models. *J. Turbomach.* **2000**, *122*, 558–569. [CrossRef]

36. Acharya, S.; Tyagi, M.; Hoda, A. Flow and heat transfer predictions for film cooling. *Ann. N. Y. Acad. Sci.* **2001**, *934*, 110–125. [CrossRef] [PubMed]

37. Azzi, A.; Jubran, B.A. Numerical modeling of film cooling from short length stream-wise injection holes. *Heat Mass Transf.* **2003**, *39*, 345–353. [CrossRef]

38. Harrison, K.L.; Bogard, D.G. Comparison of RANS turbulence models for prediction of film cooling performance. In Proceedings of the ASME Turbo Expo 2008: Power for Land, Sea, and Air, Berlin, Germany, 9–13 June 2008; Volume 43147, pp. 1187–1196.

39. Li, X.; Ren, J.; Jiang, H. Application of algebraic anisotropic turbulence models to film cooling flows. *Int. J. Heat Mass Transf.* **2015**, *91*, 7–17. [CrossRef]

40. Ling, J.; Ryan, K.J.; Bodart, J.; Eaton, J.K. Analysis of turbulent scalar flux models for a discrete hole film cooling flow. *J. Turbomach.* **2016**, *138*, 011006. [CrossRef]

41. Laschet, G.; Rex, S.; Bohn, D.; Moritz, N. 3-D conjugate analysis of cooled coated plates and homogenization of their thermal properties. *Numer. Heat Transf. Part A Appl.* **2002**, *42*, 91–106. [CrossRef]

42. Baldwin, B.; Lomax, H. Thin-layer approximation and algebraic model for separated turbulentflows. In Proceedings of the 16th Aerospace Sciences Meeting, Huntsville, AL, USA, 16–18 January 1978; p. 257.

43. Bohn, D.; Krewinkel, R. Numerical investigation of the effectiveness of effusion cooling for plane multi-layer systems with different base-materials. *Front. Energy Power Eng. China* **2009**, *3*, 406–413. [CrossRef]

44. Ceccherini, A.; Facchini, B.; Tarchi, L.; Toni, L. Adiabatic and overall effectiveness measurements of an effusion cooling array for turbine endwall application. In Proceedings of the ASME Turbo Expo 2008: Power for Land, Sea, and Air, Berlin, Germany, 9–13 June 2008.

45. Ceccherini, A.; Facchini, B.; Tarchi, L.; Toni, L.; Coutandin, D. Combined effect of slot injection, effusion array and dilution hole on the heat transfer coefficient of a real combustor liner. In Proceedings of the ASME Turbo Expo 2009: Power for Land, Sea and Air, Orlando, FL, USA, 8–12 June 2009.

46. Andreini, A.; Ceccherini, A.; Facchini, B.; Coutandin, D. Combined effect of slot injection, effusion array and dilution hole on the heat transfer coefficient of a real combustor liner part 2: Numerical analysis. In Proceedings of the ASME Turbo Expo 2010: Power for Land, Sea and Air, Glasgow, UK, 14–18 June 2010.

47. Coletti, F.; Benson, M.J.; Ling, J.; Elkins, C.J.; Eaton, J.K. Turbulent transport in an inclined jet in crossflow. *Int. J. Heat Fluid Flow* **2013**, *43*, 149–160. [CrossRef]

48. Andrei, L.; Andreini, A.; Bianchini, C.; Caciolli, G.; Facchini, B.; Mazzei, L.; Picchi, A.; Turrini, F. Effusion Cooling Plates for Combustor Liners: Experimental and Numerical Investigations on the Effect of Density Ratio. *Energy Procedia* **2014**, *45*, 1402–1411. [CrossRef]

49. Ledezma, G.A.; Lachance, J.; Wang, G.; Wang, A.; Laskowski, G.M. Experimental and Numerical Investigation of Effusion Cooling for High Pressure Turbine Components: Part 2—Numerical Results. In *Turbo Expo: Power for Land, Sea, and Air, Proceedings of the ASME Turbo Expo 2016: Turbomachinery Technical Conference and Exposition, Seoul, South Korea, 13–17 June 2016*; American Society of Mechanical Engineers: New York, NY, USA, 2016; Volume 49798, p. V05BT17A002.

50. Krawciw, J. Optimisation Techniques for Combustor Wall Cooling. Ph.D. Thesis, Loughborough University, Loughborough, UK, 2017.

51. Launder, B.; Spalding, D. The numerical computation of turbulent flows. *Comput. Methods Appl. Mech. Eng.* **1974**, *3*, 269–289. [CrossRef]

52. Pietrzyk, J.R.; Bogard, D.G.; Crawford, M.E. Effects of density ratio on the hydrodynamics of film cooling. *J. Turbomach.* **1990**, *112*, 437–443. [CrossRef]

53. Pietrzyk, J.R.; Bogard, D.G.; Crawford, M.E. Hydrodynamic measurements of jets in crossflow for gas turbine film cooling applications. *J. Turbomach.* **1989**, *111*, 139–145. [CrossRef]

54. Quarmby, A.; Quirk, R. Measurements of the radial and tangential eddy diffusivities of heat and mass in turbulent flow in a plain tube. *Int. J. Heat Mass Transf.* **1972**, *15*, 2309–2327. [CrossRef]

55. Quarmby, A.; Quirk, R. Axisymmetric and non-axisymmetric turbulent diffusion in a plain circular tube at high Schmidt number. *Int. J. Heat Mass Transf.* **1974**, *17*, 143–147. [CrossRef]

56. Bodart, J.; Coletti, F.; Bermejo-Moreno, I.; Eaton, J.K. High-fidelity simulation of a turbulent inclined jet in a crossflow. *Cent. Turbul. Res. Annu. Res. Briefs* **2013**, *19*, 263–275.

57. Roy, S.; Kapadia, S.; Heidmann, J.D. Film Cooling Analysis Using DES Turbulence Model. In Proceedings of the Turbo Expo: Power for Land, Sea, and Air, Atlanta, GA, USA, 16–19 June 2003; Volume 6: Turbo Expo 2003, Parts A and B, pp. 1113–1122. [CrossRef]

58. Foroutan, H.; Yavuzkurt, S. Numerical Simulations of the Near-Field Region of Film Cooling Jets Under High Free Stream Turbulence: Application of RANS and Hybrid URANS/Large Eddy Simulation Models. *J. Heat Transf.* **2015**, *137*, 011701. [CrossRef]

59. Jin, Y.; Lu, L.; Huang, Z.; Han, X. Numerical investigation of flat-plate film cooling using Very-Large Eddy Simulation method. *Int. J. Therm. Sci.* **2022**, *171*, 107263. [CrossRef]

60. Zamiri, A.; You, S.J.; Chung, J.T. Large eddy simulation of unsteady turbulent flow structures and film-cooling effectiveness in a laidback fan-shaped hole. *Aerosp. Sci. Technol.* **2020**, *100*, 105793. [CrossRef]

61. Mazzei, L.; Andreini, A.; Facchini, B.; Turrini, F. Impact of Swirl Flow on Combustor Liner Heat Transfer and Cooling: A Numerical Investigation With Hybrid Reynolds-Averaged Navier–Stokes Large Eddy Simulation Models. *J. Eng. Gas Turbines Power* **2015**, *138*, 051504. [CrossRef]

62. Mazzei, L.; Picchi, A.; Andreini, A.; Facchini, B.; Vitale, I. Unsteady Computational Fluid Dynamics Investigation of Effusion Cooling Process in a Lean Burn Aero-Engine Combustor. *J. Eng. Gas Turbines Power* **2016**, *139*, 011502. [CrossRef]

63. Lenzi, T.; Palanti, L.; Picchi, A.; Bacci, T.; Mazzei, L.; Andreini, A.; Facchini, B. Time-Resolved Flow Field Analysis of Effusion Cooling System With Representative Swirling Main Flow. *J. Turbomach.* **2020**, *142*, 061008. [CrossRef]

64. Arroyo-Callejo, G.; Laroche, E.; Millan, P.; Leglaye, F.; Chedevergne, F. Numerical Investigation of Compound Angle Effusion Cooling Using Differential Reynolds Stress Model and Zonal Detached Eddy Simulation Approaches. *J. Turbomach.* **2016**, *138*, 101001. [CrossRef]

65. Zhang, C.; Lin, Y.; Xu, Q.; Liu, G.; Song, B. Cooling effectiveness of effusion walls with deflection hole angles measured by infrared imaging. *Appl. Therm. Eng.* **2009**, *29*, 966–972. [CrossRef]

66. Tyagi, M.; Acharya, S. Large eddy simulation of film cooling flow from an inclined cylindrical jet. *J. Turbomach.* **2003**, *125*, 734–742. [CrossRef]

67. Iourokina, I.; Lele, S. Towards large eddy simulation of film-cooling flows on a model turbine blade with free-stream turbulence. In Proceedings of the 43rd AIAA Aerospace Sciences Meeting and Exhibit, Reno, NV, USA, 10–13 January 2005; p. 670.

68. Lund, T.S.; Wu, X.; Squires, K.D. Generation of turbulent inflow data for spatially-developing boundary layer simulations. *J. Comput. Phys.* **1998**, *140*, 233–258. [CrossRef]

69. Renze, P.; Schroder, W.; Meinke, M. Large-eddy simulation of film cooling flows with variable density jets. *Flow Turbul. Combust.* **2008**, *80*, 119–132. [CrossRef]

70. Renze, P.; Schroder, W.; Meinke, M. Large-eddy simulation of film cooling flows at density gradients. *Int. J. Heat Fluid Flow* **2008**, *29*, 18–34. [CrossRef]

71. Guo, X.; Schröder, W.; Meinke, M. Large-eddy simulations of film cooling flows. *Comput. Fluids* **2006**, *35*, 587–606. [CrossRef]

72. Rozati, A.; Tafti, D.K. Effect of coolant–mainstream blowing ratio on leading edge film cooling flow and heat transfer–LES investigation. *Int. J. Heat Fluid Flow* **2008**, *29*, 857–873. [CrossRef]

73. Vreman, A.W. An eddy-viscosity subgrid-scale model for turbulent shear flow: Algebraic theory and applications. *Phys. Fluids* **2004**, *16*, 3670–3681. [CrossRef]

74. Xie, Z.; Castro, I.P. Efficient generation of inflow conditions for large eddy simulation of street-scale flows. *Flow. Turbul. Combust.* **2008**, *81*, 449–470. [CrossRef]

75. Oliver, T.A.; Bogard, D.G.; Moser, R.D. Large eddy simulation of compressible, shaped-hole film cooling. *Int. J. Heat Mass Transf.* **2019**, *140*, 498–517. [CrossRef]

76. Immer, M.C. Time-Resolved Measurement and Simulation of Local Scale Turbulent Urban Flow. Ph.D. Thesis, ETH Zurich, 2016.

77. Kang, Y.S.; Rhee, D.H.; Song, Y.J.; Kwak, J.S. Large Eddy Simulations on film cooling flow behaviors with upstream turbulent boundary layer generated by circular cylinder. *Energies* **2021**, *14*, 7227. [CrossRef]

78. Hao, M.; di Mare, L. Reynolds stresses and turbulent heat fluxes in fan-shaped and cylindrical film cooling holes. *Int. J. Heat Mass Transf.* **2023**, *214*, 124324. [CrossRef]

79. Hao, M.; di Mare, L. Heat transfer and turbulent heat flux budgets in cooling films. *Int. J. Heat Mass Transf.* **2023**, *217*, 124687. [CrossRef]

80. Hao, M.; di Mare, L. Budgets of Reynolds stresses in film cooling with fan-shaped and cylindrical holes. *Phys. Fluids* **2023**, *35*. [CrossRef]

81. Hao, M.; Hope-Collins, J.; di Mare, L. Generation of turbulent inflow data from realistic approximations of the covariance tensor. *Phys. Fluids* **2022**, *34*, 115140. [CrossRef]

82. Mendez, S.; Nicoud, F. Large-eddy simulation of a bi-periodic turbulent flow with effusion. *J. Fluid Mech.* **2008**, *598*, 27–65. [CrossRef]

83. Renze, P.; Schro¨der, W.; Meinke, M. Large-eddy simulation of interacting film cooling jets. In Proceedings of the Turbo Expo: Power for Land, Sea, and Air, Orlando, FL, USA, 8–12 June 2009; Volume 48845, pp. 81–90.

84. Motheau, E.; Lederlin, T.; Florenciano, J.L.; Bruel, P. LES investigation of the flow through an effusion-cooled aeronautical combustor model. *Flow Turbul. Combust.* **2012**, *88*, 169–189. [CrossRef]

85. Smirnov, A.; Shi, S.; Celik, I. Random Flow Generation Technique for Large Eddy Simulations and Particle-Dynamics Modeling . *J. Fluids Eng.* **2001**, *123*, 359–371. [CrossRef]

86. Konopka, M.; Jessen, W.; Meinke, M.; Schröder, W. Large-eddy simulation of film cooling in an adverse pressure gradient flow. *J. Turbomach.* **2013**, *135*, 031031. [CrossRef]

87. El-Askary, W.; Schroeder, W.; Meinke, M. LES of compressible wall-bounded flows. In Proceedings of the 16th AIAA Computational Fluid Dynamics Conference, Orlando, FL, USA, 23–26 June 2003; p. 3554.

88. Sung, Y.; Dord, A.L.; Laskowski, G.M.; Shunn, L.; Natsui, G.; Kapat, J. Detailed large eddy simulations (LES) of multi-hole effusion cooling flow for gas turbines. In *Turbo Expo: Power for Land, Sea, and Air, Proceedings of the ASME Turbo Expo 2016: Turbomachinery Technical Conference and Exposition, Seoul, South Korea, 13–17 June 2016*; American Society of Mechanical Engineers: New York, NY, USA, 2016; Volume 49798, p. V05BT17A017.

89. Moin, P.; Squires, K.; Cabot, W.; Lee, S. A dynamic subgrid-scale model for compressible turbulence and scalar transport. *Phys. Fluids A Fluid Dyn.* **1991**, *3*, 2746–2757. [CrossRef]

90. Vreman, B.; Geurts, B.; Kuerten, H. On the formulation of the dynamic mixed subgrid-scale model. *Phys. Fluids* **1994**, *6*, 4057–4059. [CrossRef]

91. Lavrich, P.L.; Chiappetta, L.M. *An Investigation of Jet in a Cross Flow for Turbine Film Cooling Applications*; UTRC Report; United Technologies Research Center: East Hartford, CT, USA 1990.

92. Iourokina, I.; Lele, S. Large eddy simulation of film-cooling above the flat surface with a large plenum and short exit holes. In Proceedings of the 44th AIAA Aerospace Sciences Meeting and Exhibit, Reno, NV, USA, 9–12 January 2006; p. 1102.

93. Iourokina, I.V.; Lele, S.K. Large eddy simulation of film cooling flow above a flat plate from inclined cylindrical holes. In Proceedings of the Fluids Engineering Division Summer Meeting, Miami, FL, USA, 17–20 July 2006; Volume 47500, pp. 817–825.

94. Fureby, C.; Grinstein, F. Monotonically integrated large eddy simulation of free shear flows. *AIAA J.* **1999**, *37*, 544–556. [CrossRef]

95. Jessen, W.; Schröder, W.; Klaas, M. Evolution of jets effusing from inclined holes into crossflow. *Int. J. Heat Fluid Flow* **2007**, *28*, 1312–1326. [CrossRef]

96. Klein, M.; Sadiki, A.; Janicka, J. A digital filter based generation of inflow data for spatially developing direct numerical or large eddy simulations. *J. Comput. Phy.* **2003**, *186*, 652–665. [CrossRef]

97. Wolf, P.; Staffelbach, G.; Roux, A.; Gicquel, L.; Poinsot, T.; Moureau, V. Massively parallel LES of azimuthal thermo-acoustic instabilities in annular gas turbines. *Comptes Rendus Mec.* **2009**, *337*, 385–394. [CrossRef]

98. Hay, N.; Lampard, D.; Saluja, C. Effects of the condition of the approach boundary layer and of mainstream pressure gradients on the heat transfer coefficient on film-cooled surfaces. *J. Eng. Gas Turbines Power.* **1985**, *107*, 99–104. [CrossRef]

99. Ham, F. An efficient scheme for large eddy simulation of low-Ma combustion in complex configurations. *Annu. Res. Briefs Cent. Turbul. Res. Stanf. Univ.* **2007**, 41–45.

100. Duraisamy, K.; Spalart, P.R.; Rumsey, C.L. *Status, Emerging Ideas and Future Directions of Turbulence Modeling Research in Aeronautics*; Technical Report NF1676L-28239, NASA Technical Reports Server: NTRS; U.S. National Aeronautics and Space Administration: Washington, DC, USA, 2017.

101. Ling, J.; Ruiz, A.; Lacaze, G.; Oefelein, J. Uncertainty analysis and data-driven model advances for a jet-in-crossflow. *J. Turbomach.* **2017**, *139*, 021008 [CrossRef]

102. Milani, P.M.; Ling, J.; Saez-Mischlich, G.; Bodart, J.; Eaton, J.K. A machine learning approach for determining the turbulent diffusivity in film cooling flows. *J. Turbomach.* **2017**, *140*, 021006. [CrossRef]

103. Milani, P.M.; Ling, J.; Eaton, J.K. Physical interpretation of machine learning models applied to film cooling flows. *J. Turbomach.* **2019**, *141*, 011004. [CrossRef]

104. Milani, P.M.; Ling, J.; Eaton, J.K. Generalization of machine-learned turbulent heat flux models applied to film cooling flows. *J. Turbomach.* **2020**, *142*, 011007. [CrossRef]

105. Milani, P.M.; Ling, J.; Eaton, J.K. Turbulent scalar flux in inclined jets in crossflow: Counter gradient transport and deep learning modelling. *arXiv* **2020**, arXiv:2001.04600.

106. Ellis, C.D.; Xia, H. LES Informed Data-driven Models for RANS Simulations of Single-hole Cooling Flows. *Int. J. Heat Mass Trans.* **2024**. [CrossRef]

107. Milani, P.M.; Ling, J.; Eaton, J.K. On the generality of tensor basis neural networks for turbulent scalar flux modeling. *Int. Commun. Heat Mass* **2021**, *128*, 105626. [CrossRef]

108. Wang, C.; Liu, Y.; Zhang, J. Prediction of thermo-mechanical performance for effusion cooling by machine learning method. *Int. J. Heat Mass Transf.* **2023**, *207*, 123969. [CrossRef]

109. Yang, L.; Dai, W.; Rao, Y.; Chyu, M.K. A machine learning approach to quantify the film cooling superposition effect for effusion cooling structures. *Int. J. Therm. Sci.* **2021**, *162*, 106774. [CrossRef]

110. Yu, H.; Lou, J.; Liu, H.; Chu, Z.; Wang, Q.; Yang, L.; Rao, Y. A transfer learning method to assimilate numerical data with experimental data for effusion cooling. *Appl. Therm. Eng.* **2023**, *224*, 120075. [CrossRef]

111. Paccati, S.; Mazzei, L.; Andreini, A.; Facchini, B. Reduced-order models for effusion modeling in gas turbine combustors. *J. Turbomach.* **2022**, *144*, 081013. [CrossRef]

112. Huang, W.; Zhang, X.; Zhou, W.; Liu, Y. Learning time-averaged turbulent flow field of jet in crossflow from limited observations using physics-informed neural networks. *Phys. Fluids* **2023**, *35*, 025131. [CrossRef]

113. Huang, W.; Zhang, X.; Shao, H.; Chen, W.; He, Y.; Zhou, W.; Liu, Y. Swirling flow field reconstruction and cooling performance analysis based on experimental observations using physics-informed neural networks. *J. Glob. Power Propuls. Soc.* **2024**, *8*, 141–153. [CrossRef]